

SPECIAL REPORT 92-7

AD-A252 014



2



Precision Analysis and Recommended Test Procedures for Mobility Measurements Made with an Instrumented Vehicle

Sally A. Shoop

April 1992

**S DTIC
ELECTE
JUN 26 1992
A D**

This document has been approved for public release and sale; its distribution is unlimited.

92-16757



92 6 25 043

For conversion of SI metric units to U.S./British customary units of measurement consult ASTM Standard E380, Metric Practice Guide, published by the American Society for Testing and Materials, 1916 Race St., Philadelphia, Pa. 19103.

This report is printed on paper that contains a minimum of 50% recycled material.



**U.S. Army Corps
of Engineers**
Cold Regions Research &
Engineering Laboratory

Precision Analysis and Recommended Test Procedures for Mobility Measurements Made with an Instrumented Vehicle

Sally A. Shoop

April 1992



| | |
|--------------------|-------------------------------------|
| Accession For | |
| NTIS CRA&I | <input checked="" type="checkbox"/> |
| DTIC TAB | <input type="checkbox"/> |
| Unannounced | <input type="checkbox"/> |
| Justification | |
| By _____ | |
| Distribution/ | |
| Availability Codes | |
| Dist | Available for Special |
| A-1 | |

Prepared for
OFFICE OF THE CHIEF OF ENGINEERS

Approved for public release, distribution is unlimited.

PREFACE

This report was prepared by Sally A. Shoop, Research Civil Engineer, of the Applied Research Branch, Experimental Engineering Division, U. S. Army Cold Regions Research and Engineering Laboratory. Funding for this research was provided by DA Project 4A762784AT42, *Design, Construction and Operations Technology for Cold Regions*, Task CS, Work Unit 007, *Off-road Mobility in Thawing Soils*.

The author thanks the following individuals who helped collect and reduce the data used in this study: Rosanne Stoops, Stephen Decato, Andrew Sundelin, Paul Richmond, and Heather Banker. She also thanks Paul Richmond, George Blaisdell, Beth Berliner, Dr. C.L. Grant, Susan Taylor and Edmund Wright for their thoughtful reviews of the text.

CONTENTS

| | |
|---|----|
| Preface | ii |
| Introduction | 1 |
| Statistical considerations | 1 |
| Background on mobility testing | 3 |
| Instrumentation configuration of the CRREL Instrumented Vehicle (CIV) | 3 |
| Vehicle calibration | 4 |
| Typical mobility test procedures | 4 |
| Experimental error | 4 |
| Systematic errors | 7 |
| Vehicle calibration method | 10 |
| Temperature | 14 |
| Vehicle speed | 18 |
| Contact patch area | 21 |
| Discussion and application to experimental programs | 22 |
| Summary and conclusions | 25 |
| Literature cited | 26 |
| Appendix A: Range test for homogeneity of variance | 27 |
| Abstract | 49 |

ILLUSTRATIONS

Figure

| | |
|---|----|
| 1. Influence of experimental error on ability to detect variable effects | 2 |
| 2. CRREL Instrumented Vehicle | 3 |
| 3. Axis convention for triaxial load cells mounted on the front wheels of the instrumented vehicle | 3 |
| 4. Distribution of hard surface rolling resistance measured at the left wheel as shown on probability paper | 5 |
| 5. Distribution of hard surface rolling resistance measured at the right wheel as shown on probability paper | 6 |
| 6. Bar graph comparing the standard deviations of the zero values for each channel, obtained using the three calibration methods | 13 |
| 7. Bar graph comparing the standard deviations of the zero values for each channel, obtained using the three calibration methods | 13 |
| 8. Location of the thermocouples on the instrumented vehicle | 14 |
| 9. Temperatures measured at the load cells and the ambient temperature measured on 18 October | 15 |
| 10. Temperatures measured at the load cells and the ambient temperature measured on October 19 | 15 |
| 11. Load cell and velocity zero readings vs average temperature at the load cell | 16 |
| 12. Rolling resistance vs speed | 20 |
| 13. Hard surface motion resistance vs vehicle speed | 20 |
| 14. Hard surface motion resistance vs vehicle speed | 21 |
| 15. Hard surface motion resistance vs vehicle speed | 22 |
| 16. Tire contact areas at various vehicle load conditions | 23 |
| 17. Tire contact areas at various vehicle load conditions | 23 |
| 18. Operating characteristics curves for a two-tailed <i>t</i> -test with 95% confidence | 24 |
| 19. Mobility testing checklist | 26 |

TABLES

Table

| | |
|--|---|
| 1. Resistance values for hard surface rolling resistance for the same tire at 26-psi inflation pressure using a rolling calibration | 5 |
| 2. Standard deviation from traction tests performed on a variety of terrain conditions | 7 |

| | |
|---|----|
| 3. Comparison of hard surface rolling resistance measurements | 8 |
| 4. Standard deviation of resistance data measured for many different experimental conditions | 9 |
| 5. Zero values for each channel from the instrumented vehicle for the series of calibration tests taken on October 18, 1989 | 11 |
| 6. Zero values for each channel from the instrumented vehicle for the series of calibration tests taken on October 19, 1989 | 12 |
| 7. Results of rolling resistance measured at different speeds | 17 |
| 8. Results of rolling resistance measured at different speeds | 18 |
| 9. Results of rolling resistance measured at different speeds | 19 |
| 10. Deflection from weight on bumper at two tire pressures | 23 |

Precision Analysis and Recommended Test Procedures for Mobility Measurements Made with an Instrumented Vehicle

SALLY A. SHOOP

INTRODUCTION

In the past, CRREL's mobility research program concentrated on mobility on snow and ice where the effects of the variables being studied (snow type and traction aids) were quite large and relative changes in mobility were easily detected. More recent research interests, however, include mobility on shallow snow and freezing/thawing ground where the effects of the terrain and tire variables are more subtle. When the quantities being measured are small relative to the noise, scatter in the data can be detrimental to the success of the experiment.

This report documents the precision and reproducibility of mobility measurement with an instrumented vehicle. The experiments were performed over several years and their goal was to isolate and quantify causes of variability in measurements occurring during normal mobility testing operations. Statistical methods were used to determine how different variables were systematically affecting the data. This analysis allowed us to improve the precision of mobility testing and made the measurement of more subtle effects possible.

STATISTICAL CONSIDERATIONS

In any experimental program it is important to know the precision of the experimental procedure. This knowledge is used to maximize the results obtained and minimize the time and cost of an experimental program. The precision, or experimental error, includes the repeatability of the measurements (agreement of results obtained with the same method, on identical test material and under the same conditions) as well as how reproducible these measurements are under different conditions (when measured by different operators, at a different time or with a different apparatus). Experimental error consists of both random error and systematic error, sometimes call bias error. Random error is dealt with by replicating experiments and calculating an

average because the average value of random error is zero. (If the data set is small, the average value of the random error only approximates zero.) Random experimental error can be expressed by the standard deviation, sometimes also called standard error, which is a measurement of precision. Systematic error, however, will bias the experimental results and must be eliminated or accounted for. Systematic errors are eliminated by improvements in technique, correction to the data, or reduction of their biasing by randomization.

Some scatter exists in any experimental data but if the effects of the variables (such as snow depth) are large, relative changes in results (such as vehicle motion resistance) are easily detected. This type of situation is illustrated in Figure 1a, which shows how experimental error influences whether the effects of an experimental factor can be detected. In this figure the horizontal axis represents values of a "factor," which is statistical jargon for independent variable, such as properties that characterize the terrain or vehicle. Responses are the dependent variables we measure, such as traction or motion resistance, and these are represented on the vertical axis. Experimental error is the reproducibility of the response measurement and is commonly expressed as the standard deviation. The "effect" is the change in a response caused by a change in a factor.

Because of the strong effect of snow on the magnitude of the vehicle motion resistance, relative changes in resistance are easily detected, even if the experimental error is relatively large, as shown in Figure 1a. However, for motion resistance on shallow snow and frozen/thawing ground the forces measured can be small and the effects of the terrain subtle. Thus, the scatter in the data is more apparent, and can be detrimental to the success of the experimental program as indicated in Figure 1b where the effect is smaller than the experimental error and much more difficult to detect.

To successfully detect the small effects caused by some variables the experimental program must be carefully planned. The uncertainty must be decreased or the range of the test variable (factor) must be large. The

precision of the measurement can be improved (experimental error decreased) by refining the experimental technique to eliminate systematic errors or by increasing the number of replicate tests. The relationship between the experimental standard deviation and number of replicates is

$$S_{\bar{y}} = S_y / \sqrt{n} \quad (1)$$

where $S_{\bar{y}}$ = the standard deviation of the mean

S_y = the standard deviation of the individual measurements

n = the number of replicates

However, since the uncertainty (standard deviation of the mean) is reduced by $1 / \sqrt{n}$, improvements are only minor above $n = 5$.

Using hypothesis testing, we can estimate the number of replicates needed to detect an effect of size δ at some stated confidence level from

$$n = \frac{t^2 S_y^2}{\delta^2} \quad (2)$$

where δ is the size of the effect and t is the value from Student's t test, which takes into account uncertainties in the estimate of the standard deviation. From this equation you can see how a decrease in the standard deviation will decrease the number of replicates needed. This will reduce the time and cost of the experimental program. Or, if the standard deviation and the number of replicates are known, eq 2 can be used to estimate the minimum detectable effect. The relationships between

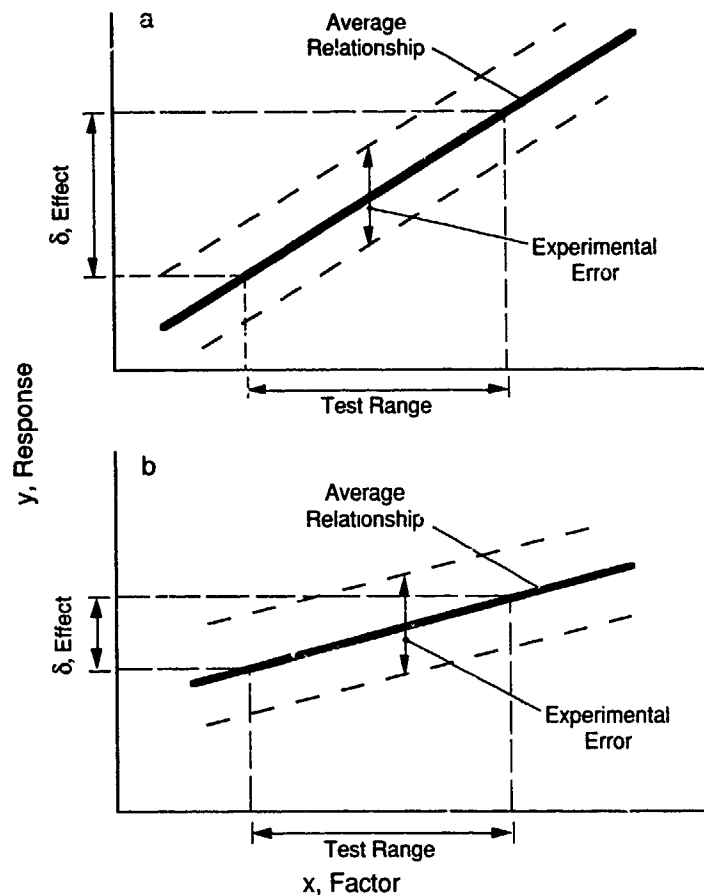


Figure 1. Influence of experimental error on ability to detect variable effects. If the variable effect is large (i.e., a steep slope on the graph) then it can be detected even when experimental error is relatively large (case 1a). If the effect is small, experimental error must be reduced to aid in detecting the effect experimentally (case 1b)



Figure 2 CRREL Instrumented Vehicle.

these parameters (size of detectable effect, standard deviation, number of replicates, confidence and risk) are discussed fully in Natrella (1963) among other references on experimental statistics.

BACKGROUND ON MOBILITY TESTING

Instrumentation configuration of the CRREL Instrumented Vehicle (CIV)

Although the data were collected using an instrumented vehicle, the test techniques, analysis and results

are applicable to mobility testing in general. To understand the nature of the mobility measurements, a brief description of the test vehicle (Fig. 2) and the different mobility test procedures used will be presented.

Currently, each of the front wheels of the vehicle is instrumented to measure the forces at the tire/ground interface and the speed of each wheel. (All four wheels were instrumented in 1991.) The load cells measure forces in three perpendicular directions: longitudinal (in the direction of travel), vertical, and transverse (side forces, generated during turning maneuvers), as shown in Figure 3. Although the load cells are mounted along

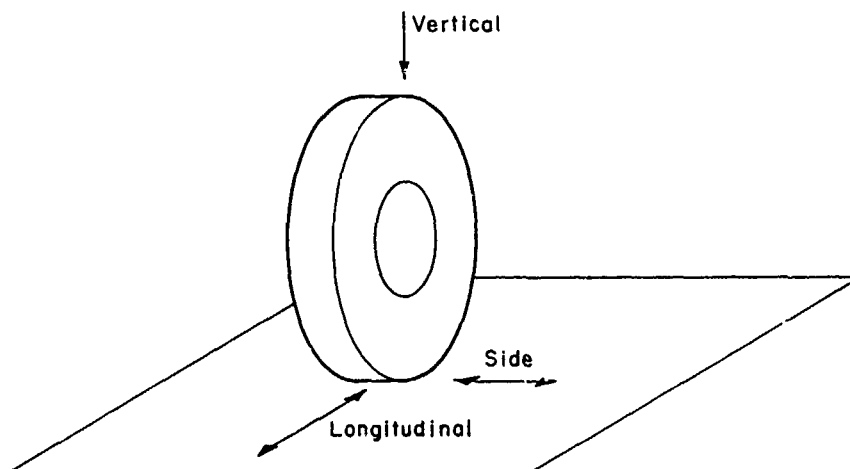


Figure 3. Axis convention for triaxial load cells mounted on the front wheels of the instrumented vehicle.

the axles, they actually measure the forces generated at the interface between the wheel and the ground, through the response of the axle. The speed of each wheel is measured using a proximity gauge and counter and the vehicle speed is measured using a fifth wheel or a sonic sensor. The instrumentation of the CIV is fully detailed in Berliner and Shoop (1991) and Blaisdell (1983).

Vehicle calibration

The vehicle should be "calibrated" at the beginning of each test series and again if it is turned off, if the conditions change significantly, or if the tests take over three hours to complete. In the past, the standard calibration method was to turn on the vehicle and all electrical components and allow them to warm up for at least 15 minutes. The front of the vehicle was then jacked clear of the ground so that the wheels were free from load. In this position, the vertical channel of the load cells was read and equated to zero load. The vehicle was then lowered, rolled back and forth to remove any unusual offset in the suspension caused when lowering the vehicle, and then rolled to a stop, without braking, while in neutral. In this position, the horizontal (longitudinal and side) channels of the load cells were read and stored as zero load values. Zeroing at this position factors out the stresses on the wheels caused by the vehicle suspension and by deflected belts and cords in the tires. In both the elevated and on-ground positions, readings are also taken with precision shunt resistors across the appropriate load cell channels. Zero velocity is read while the vehicle is motionless and is scaled by taking readings while driving the vehicle at a given constant speed, usually 5 mph.

Typical mobility test procedures

A mobility test sequence generally consists of both traction and motion resistance tests. To measure traction, the vehicle is driven at a constant speed (generally 3 to 5 mph) in front wheel drive. The speed of the front wheels is then gradually increased (either manually or automatically using a stepper motor) while the brakes are applied to the rear wheels to hold the vehicle speed constant. The resulting slip of the front wheels is usually reported as the wheel-to-ground differential interface velocity (DIV) which is equal to the speed of the wheel minus the speed of the vehicle. Traction is generally reported as a tractive coefficient (longitudinal force divided by vertical force) and is plotted as a function of the DIV.

Motion resistance is determined by measuring the longitudinal force on the front wheels with the vehicle in rear-wheel drive. Again, the vehicle is operated at a constant speed. Motion resistance is reported as the average longitudinal force or as a motion resistance

coefficient (longitudinal divided by vertical force). The motion resistance on deformable terrain is sometimes reported as terrain resistance (also called external resistance), which is that part of the motion resistance caused by the terrain deformation only (i.e., does not include the effects of the deformation or flexing of the running gear). Terrain resistance is calculated by subtracting the motion resistance measured on a hard surface from the total motion resistance measured on the deformable terrain. The hard surface motion resistance is generally measured on a paved road near the test area.

EXPERIMENTAL ERROR

Knowledge of the standard deviation, a measure of experimental error, is needed to determine the magnitude of the effect that can be measured. If the true standard deviation is unknown, as is usually the case, an estimate can be made from previous data of a similar nature. (If absolutely no data exist an estimate can be made using rules of thumb presented in Natrella [1963].) CRREL vehicle mobility measurements taken over the last several years have been used to estimate the standard deviation.

First, the data were checked to determine if the assumptions regarding the application of certain statistical techniques were valid, i.e., if the data are normally distributed. To check the distribution of the data, a data set of hard surface motion resistance values collected during November and December of 1988 and 1989 was plotted on probability paper. To do this, the resistance values are arranged in ascending order. The first value is assigned a probability of $P = 100/2n$ and each following value is assigned a probability of $P_i = P_{i-1} + 100/n$, where n is the number of values (Table 1). The values are then plotted against the probability, using probability paper, as shown in Figures 4 and 5, and should fall along a line if the data are normally distributed. By visually fitting the data with a line we can graphically estimate the mean (50% probability) and the standard deviation (the difference between the values at 50% and 84% probability). The good agreement between graphical values of mean and standard deviation obtained from Figures 4 and 5 and the values calculated from Table 1 indicates that the assumption of a normal distribution is correct. Even if the distribution is only approximately normal, most statistical techniques are still applicable: the statistical techniques are said to be robust to nonnormality.

Since we have many traction and motion resistance measurements taken over the years, but they are taken in small sets for each different terrain condition, a good estimate of the precision of our measurements can be

Table 1. Resistance values for hard surface rolling resistance for the same tire at 26-psi inflation pressure using a rolling calibration.

Values from the left and right wheel are sorted in ascending order and assigned a probability value for plotting the distribution on probability paper. The agreement between the calculated and graphical average and standard deviation indicates that the data are normally distributed.

| Sort left | | Sort right | | Probability value |
|------------------------|------|------------------------|-------|-------------------|
| Test | Left | Test | Right | |
| 1988 1223A | 9.7 | 1988 1223A | 7.9 | 3.85 |
| 1989 1116A | 4.7 | 1988 1216A | 4.5 | 11.54 |
| 1988 1216A | 4.4 | 1989 1117A | 3.8 | 19.28 |
| 1989 1115A | 4.1 | 1988 1106A | 3.3 | 26.97 |
| 1988 1226A | 3.9 | 1988 1224A | 2.9 | 34.66 |
| 1988 1224A | 3.8 | 1988 1106B | 2.4 | 42.35 |
| 1988 1106B | 2.7 | 1988 1226A | 2.0 | 49.98 |
| 1989 1117A | 2.6 | 1989 1115A | 1.9 | 57.67 |
| 1988 1106A | 1.8 | 1989 1103A | 1.2 | 65.36 |
| 1989 1103A | 0.0 | 1989 1116A | 1.1 | 73.05 |
| 1989 1107A | -1.6 | 1988 1105A | -2.7 | 80.75 |
| 1989 1120A | -1.8 | 1989 1107A | -2.9 | 88.44 |
| 1988 1105A | -4.4 | 1989 1120A | -3.6 | 96.13 |
| Calc avg | 2.30 | Calc avg | 1.68 | |
| Calc std | 3.6 | Calc std | 3.2 | |
| Graphical avg (Fig. 4) | 2.5 | Graphical avg (Fig. 5) | 1.5 | |
| Graphical std (Fig. 4) | 4.0 | Graphical std (Fig. 5) | 3.3 | |

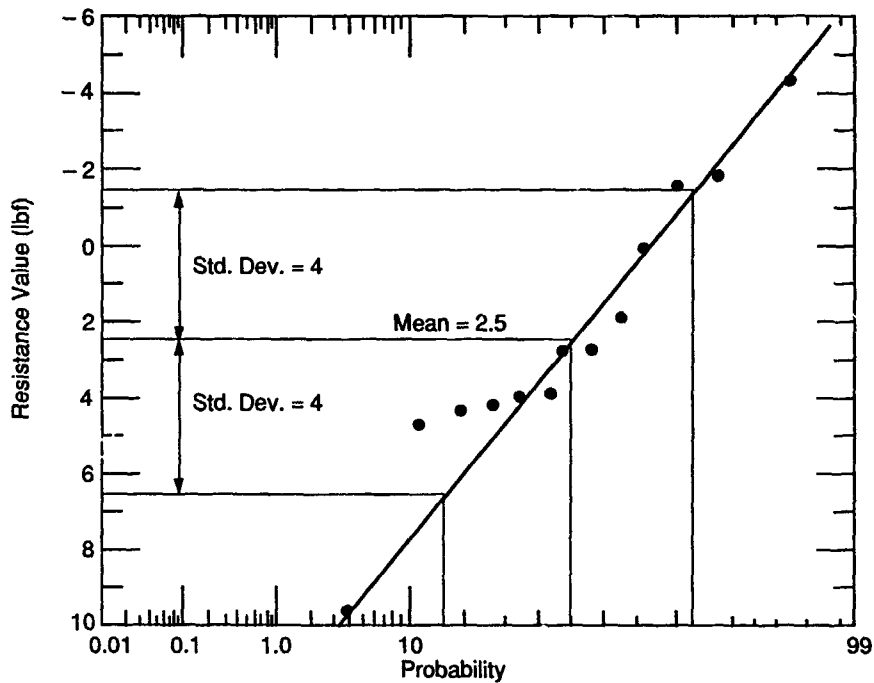


Figure 4. Distribution of hard surface rolling resistance measured at the left wheel (Table 1) as shown on probability paper. The relatively straight line along with the agreement between the calculated and graphical mean and standard deviation indicates that the data fall within a normal or Gaussian distribution.

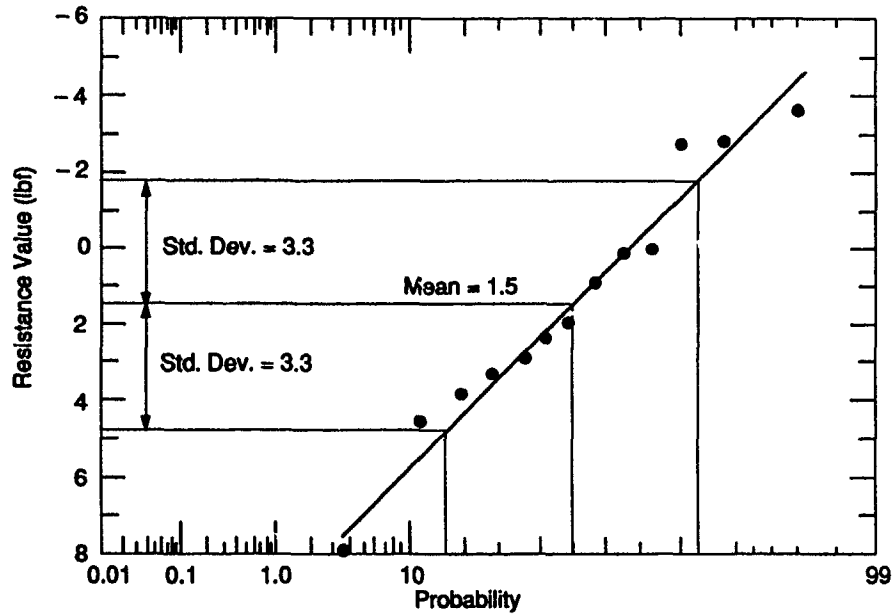


Figure 5. Distribution of hard surface rolling resistance measured at the right wheel (Table 1) as shown on probability paper. The relatively straight line along with the agreement between the calculated and graphical mean and standard deviation indicates that the data falls within a normal distribution.

obtained by pooling the standard deviations of the individual data sets. A pooled standard deviation is essentially the weighted average of the standard deviation of the separate data sets, and is obtained using the following equation:

$$S_{y \text{ pooled}} = \left[\frac{(n_i - 1) S_{y_i}^2 + (n_{i+1} - 1) S_{y_{i+1}}^2 + \dots}{(n_i - 1) + (n_{i+1} - 1) + \dots} \right]^{1/2} \quad (3)$$

where $S_{y \text{ pooled}}$ = the pooled standard deviation
 S_{y_i} = standard deviation of data set i
 n_i = number of replicates in data set i
 i = data set, $i + 1$ symbolizes next data set.

To calculate the pooled standard deviation, I used traction data from tests performed in Montana during March 1987 (Blaisdell et al. 1987). A variety of terrain conditions were tested and, for each terrain condition, several traction tests were performed. The results are expressed as a peak traction value for left and right wheels. The terrain conditions and the average and standard deviation for each data set are summarized in Table 2.

To pool the standard deviations, the data should first be checked for homogeneity, a measure of the similarity

of the standard deviations, assuming that the value of the standard deviation is similar for all data sets (or terrain conditions). A range test is used to show that the data are indeed homogeneous. A brief explanation and the calculations for the range test are shown in Appendix A along with the test data.

From eq 3, a pooled standard deviation can be calculated and used to examine our experimental designs and evaluate the probability of experimental success. The pooled standard deviation for the traction coefficient is 0.025. (The relative standard deviation, or coefficient of variation, is 6%.) This standard deviation encompasses variability due to terrain, and the influence of changing environmental conditions on the vehicle instrumentation and data acquisition (i.e., reproducibility). This value is generally adequate because the effect of changes in terrain is much greater than this, as in the case shown in Figure 1a.

Similarly, we can calculate the standard deviation of resistance data. Table 3 shows the rolling resistance on the same stretch of asphalt road measured on different dates using the same tire. Two inflation pressures are used and the mean and standard deviation are calculated for each inflation pressure. The mean and standard deviation are actually the mean and standard deviation of the average resistance calculated from each test. The bottom half of the table contains resistance values

Table 2. Standard deviation from traction tests performed on a variety of terrain conditions.
The values are based on an average of peak traction for a number of tests at each condition. The complete data set is given in Appendix A.

| Date 1987 | Conditions | Peak traction | | | | No. of tests |
|-------------------------------|-------------------------------|---------------|-------|--------------------|-------|--------------|
| | | Average | | Standard deviation | | |
| | | Left | Right | Left | Right | |
| 3/12 | Dry soil, 15 psi | 0.542 | 0.548 | 0.024 | 0.036 | 9 |
| 3/12 | Dry soil, 15 psi | 0.573 | 0.624 | 0.010 | 0.025 | 4 |
| 3/13 | Lt. rain on soil, 15 psi | 0.530 | 0.520 | 0.014 | 0.021 | 5 |
| 3/13 | 1/16 in. rain on soil, 15 psi | 0.608 | 0.595 | 0.025 | 0.023 | 5 |
| 3/17 | Dry soil, 15 psi | 0.728 | 0.720 | 0.023 | 0.040 | 6 |
| 3/17 | Dry soil, 26 psi | 0.697 | 0.701 | 0.035 | 0.026 | 6 |
| 3/17 | Dry soil, 26 psi | 0.730 | 0.727 | 0.018 | 0.025 | 6 |
| 3/19 | 7 in. snow, 26 psi | 0.289 | 0.281 | 0.038 | 0.041 | 6 |
| 3/19 | 7 in. snow, 15 psi | 0.279 | 0.307 | 0.023 | 0.031 | 5 |
| 3/19 | 10 in. snow, 15 psi | 0.319 | 0.272 | 0.024 | 0.017 | 6 |
| 3/19 | 11 in. snow, 15 psi | 0.321 | 0.219 | 0.031 | 0.016 | 6 |
| 3/21 | 6 in. snow, 15 psi | 0.412 | 0.439 | 0.014 | 0.035 | 5 |
| 3/21 | 6 in. snow, 26 psi | 0.393 | 0.350 | 0.022 | 0.012 | 8 |
| 3/21 | Slushly, 26 psi | 0.696 | 0.689 | 0.015 | 0.020 | 4 |
| 3/21 | Slushly, 15 psi | 0.664 | 0.658 | 0.018 | 0.034 | 4 |
| Sum of both wheels | | | | 4.234 | | 85 × 2 |
| S _{ypooled} | | | | 0.025 | | |
| Relative S _{ypooled} | | | | 6% | | |

obtained using a rolling calibration method, which will be discussed in more detail later.

In addition, since resistance is generally expressed as an average value of resistance measured over a certain distance (rather than a peak of a curve as in traction) we can also calculate a standard deviation for each resistance test (rather than requiring a set of tests). Since a resistance test usually contains over 100 individual measurements (based on the data acquisition rate of 10 per second), there is enough information to get a good estimate of the standard deviation (repeatability) of the measurement (S_y). The standard deviations of resistance measurements were calculated for many different experimental conditions and are given in Table 4. Standard deviation calculated in this way, however, does not include variability caused by recalibrating the test equipment or drift in the measurements occurring over time since each test takes only a very short time. Rather, it reflects the repeatability of the measurement and the variability of the terrain over the surface measured. In general, the high resistance measurements have a higher standard deviation. Of course, this depends on the lateral uniformity of the terrain and on the

roughness of the terrain surface. Because of this, the lowest standard deviations are for hard surface rolling resistance measurements taken on a smooth asphalt road, whose standard deviations are of the same order of magnitude in both Tables 3 and 4.

The standard deviations shown in Table 4 cover a wide range and most are adequate for detecting large effects over a large range (Fig. 1b). But for evaluating the effects of variables that have a smaller effect on resistance, either the range of the variable must be increased, the number of replicates increased, or the standard deviation decreased, as indicated in eq 2. The remainder of this report concentrates on decreasing the standard deviation (improving the precision) of our mobility measurements in order to examine the effects of some of these other terrain variables.

SYSTEMATIC ERRORS

To reduce the experimental error, the test technique must be improved by finding and eliminating systematic and random errors in the data. Aside from the

Table 3. Comparison of hard surface rolling resistance measurements.

All data are for the same tire at two different inflation pressures. The top of the table lists data obtained from a standard static calibration and the bottom half lists data from a rolling calibration.

| <i>Average resistance (static calibration)</i> | | | | | |
|---|---------------------|----------------------|-------------|---------------------|----------------------|
| <i>Test</i> | <i>26 psi</i> | | <i>Test</i> | <i>15 psi</i> | |
| | <i>Left lbf</i> | <i>Right lbf</i> | | <i>Left lbf</i> | <i>Right lbf</i> |
| 0606D | -10.5 | -5.2 | 0315I | -43.7 | -46.9 |
| 0606E | -7.3 | -5.5 | 0316J | -45.9 | -49.0 |
| 0606F | -11.7 | -6.3 | 0610M | -38.5 | -44.7 |
| 0610A | -12.6 | -17.0 | 0610N | -37.1 | -42.6 |
| 0610B | -13.2 | -18.4 | 0610O | -35.8 | -39.5 |
| 0610C | -12.5 | -18.9 | 0719Y | -35.8 | -27.9 |
| 0720A | -16.8 | -15.1 | 0719Z | -36.5 | -26.3 |
| 0720B | -15.2 | -16.2 | 0720Q | -35.5 | -27.2 |
| 0720C | -19.0 | -14.5 | 0720S | -34.2 | -27.2 |
| | | | 0720T | -29.6 | -28.6 |
| Number of observations | 9 | 9 | — | 10 | 10 |
| Mean | -13.2 | -13.0 | — | -37.3 | -36.0 |
| Standard deviation | 3.5 | 5.7 | — | 4.6 | 9.4 |
| <i>Average resistance (rolling calibration)</i> | | | | | |
| <i>Test</i> | <i>26 psi</i> | | <i>Test</i> | <i>15 psi</i> | |
| | <i>Left lbf</i> | <i>Right lbf</i> | | <i>Left lbf</i> | <i>Right lbf</i> |
| 1103A | 0.0 | -1.2 | 1105I | -29.0 | -16.7 |
| 1107A | 1.6 | 2.9 | 1105J | -24.7 | -20.3 |
| 1115A | -4.1 | -1.9 | 1216N | -35.3 | -20.4 |
| 1116A | -4.7 | -1.1 | 1223L | -27.7 | -30.7 |
| 1117A | -2.6 | -3.8 | 1224F | -35.4 | -21.6 |
| 1120A | 1.8 | 3.8 | 1226F | -25.2 | -19.7 |
| | | | 1107H | -24.5 | -22.9 |
| | | | 1115H | -31.9 | -23.9 |
| | | | 1116G | -21.5 | -14.8 |
| | | | 1117F | -24.2 | -24.1 |
| Number of observations | 6 | 6 | — | 10 | 10 |
| Mean | -1.3 | -0.2 | — | -27.9 | -21.5 |
| Standard deviation | 2.9 | 2.9 | — | 4.9 | 4.4 |

Table 4. Standard deviation of resistance data measured for many different experimental conditions.

Each standard deviation is based on one test containing many (over 100) data points. (Snow data obtained during study by Richmond et al. 1991, thawing soils data obtained from Shoop 1989 and 1990.)

| Test no. | Conditions | Calibration | Tire type | Tire psi | Average (lbf) | | Standard deviation (lbf) | |
|----------|-----------------------------|-----------------|-----------|----------|---------------|--------|--------------------------|------|
| | | | | | L | R | L | R |
| 0719Y | Asphalt | Static | A | 15 | -35.8 | -27.9 | 4.8 | 6.1 |
| 0302D | Asphalt | Static | C | 60 | -44.0 | -61.7 | 7.8 | 6.9 |
| 0117E | Hard pack snow | Static | A | 15 | -57.1 | -48.6 | 24.3 | 10.6 |
| 0117A | Hard pack snow | Static | A | 26 | -12.6 | -11.8 | 22.5 | 13.9 |
| 0117I | Groomed snow road | Static | B | 20 | -40.3 | -31.0 | 31.1 | 14.2 |
| 0117A | Groomed snow road | Static | B | 34 | -10.4 | -19.7 | 17.7 | 16.1 |
| 0118A | 3 in snow | Static | A | 26 | -26.0 | -37.9 | 9.3 | 10.7 |
| 0118C | 3 in snow | Static | D | 36 | -36.3 | -35.7 | 19.4 | 18.6 |
| 0118B | 3 in snow | Static | C | 60 | -25.9 | -22.0 | 15.2 | 8.1 |
| 0301V | 4 in snow | Static | B | 34 | -123.8 | -118.3 | 32.3 | 26.5 |
| 03014 | 4 in snow | Static | B | 34 | -138.3 | -164.1 | 41.7 | 47.0 |
| 0119C | 5 in snow | Static | D | 26 | -49.8 | -63.4 | 19.6 | 31.8 |
| 0119A | 5 in snow | Static | A | 26 | -68.4 | -24.9 | 29.8 | 10.6 |
| 0119B | 5 in snow | Static | C | 60 | -33.1 | -1.7 | 12.6 | 9.9 |
| 0301A | 6 in snow | Static | B | 20 | -148.7 | -157.4 | 41.2 | 54.3 |
| 0120A | 6.7 in snow | Static | D | 26 | -61.7 | -70.2 | 45.1 | 44.5 |
| 0301E | 7 in snow | Static | A | 26 | -172.8 | -161.1 | 34.7 | 26.6 |
| 0302I | 7 in snow | Static | C | 60 | -186.3 | -149.4 | 42.4 | 38.7 |
| 0302H | 7.8 in snow | Static | C | 60 | -208.3 | -193.1 | 72.7 | 64.7 |
| 0301M | 7.9 in snow | Static | A | 26 | -211.1 | -190.9 | 31.2 | 27.1 |
| 0301L | 8.3 in snow | Static | A | 26 | -188.7 | -199.1 | 35.7 | 53.5 |
| 0301F | 8.7 in snow | Static | A | 15 | -185.9 | -188.9 | 37.3 | 35.4 |
| 0120C | 8.7 in snow | Static | A | 26 | -95.9 | -112.3 | 65.9 | 41.3 |
| 0302E | 9 in snow | Static | C | 60 | -252.4 | -260.3 | 91.7 | 83.0 |
| 0301P | 9.5 in snow | Static | A | 26 | -224.0 | -218.5 | 39.7 | 30.0 |
| 0302C | 10 in snow | Static | C | 60 | -130.1 | -252.6 | 29.3 | 39.6 |
| 0120B | 12 in snow | Static | C | 60 | -127.5 | -123.4 | 55.8 | 43.0 |
| 0719V | 1 in thawed sand | Static | A | 15 | -40.5 | -37.1 | 33.0 | 26.6 |
| 0719N | 1 in thawed sand | Static | A | 26 | -40.6 | -23.5 | 36.1 | 34.1 |
| 0510J | 3.5 thawed sand | Static | A | 15 | -42.8 | -34.8 | 28.4 | 24.3 |
| 0510C | 3.5 thawed sand | Static | A | 26 | -39.3 | -23.2 | 34.1 | 33.8 |
| 1101D | Asphalt | Rolling @26 psi | A | 15 | -28.1 | -24.2 | 3.1 | 3.7 |
| 1115A | Asphalt | Rolling @26 psi | A | 26 | -4.1 | -1.9 | 3.8 | 3.2 |
| 1108A | Asphalt | Rolling @35 psi | A | 35 | 6.3 | -4.7 | 6.5 | 5.7 |
| 1115L | 1/2 thawed sand | Rolling @26 psi | A | 15 | -42.9 | -38.7 | 24.0 | 16.9 |
| 1115B | 1/2 thawed sand | Rolling @26 psi | A | 26 | -24.7 | -14.6 | 36.1 | 33.0 |
| 1216G | 3.5 in thawed sand | Rolling @26 psi | A | 15 | -137.2 | -143.5 | 78.0 | 68.7 |
| 1116B | 3.5 in thawed sand | Rolling @26 psi | A | 26 | -14.6 | -4.7 | 40.9 | 23.5 |
| 1216B | 3.5 in thawed sand | Rolling @26 psi | A | 26 | -176.6 | -136.2 | 98.9 | 84.5 |
| 0327B | 3.5 in thawed sand | Rolling @26 psi | A | 26 | -28.0 | -30.8 | 33.2 | 32.6 |
| 0327B | 7 in thawed sand | Rolling @26 psi | A | 26 | -40.2 | -42.6 | 27.3 | 34.9 |
| 0327H | 12 in thawed sand | Rolling @26 psi | A | 26 | -113.9 | -132.0 | 52.0 | 49.0 |
| 1108M | 1 in thawed silt | Rolling @35 psi | A | 15 | -27.7 | 23.7 | 17.0 | 16.8 |
| 1108B | 1 in thawed silt | Rolling @35 psi | A | 35 | -7.3 | -7.1 | 20.6 | 20.0 |
| 1113S | 4 in thawed silt trafficked | Rolling @35 psi | A | 15 | -69.0 | -41.9 | 48.6 | 42.4 |
| 1113L | 4 in thawed silt trafficked | Rolling @35 psi | A | 26 | -32.8 | -26.0 | 41.9 | 36.7 |
| 1113E | 4 in thawed silt trafficked | Rolling @35 psi | A | 35 | -76.5 | -33.2 | 33.1 | 31.4 |

variability in the terrain itself, some variability in the data appears to be associated with the calibration of the vehicle. Scatter in the vehicle zero-load values, causing day-to-day variability in the readings, was identified during vehicle calibration checks. Since then, several tests were performed on the vehicle to isolate and reduce the cause of scatter in the data. Initially these tests were extremely frustrating because, while I was trying to isolate one factor, other (unknown) factors were confounding the results. After a great deal of time and effort several sources of systematic experimental error (static wheel alignment, temperature, speed, and slight variations in weight distribution) were identified. Although the effects of these parameters are within the limits of accuracy needed for some test programs, their combined effects can be large enough to be detrimental to other experiments (such as motion resistance in shallow snow). Therefore, several experiments were performed to evaluate the nature of the effect of these variables and to determine how to eliminate or correct them.

Vehicle calibration method

The most elusive variability in the data was from changes in the load cell readings while zeroing the horizontal forces of the load cell from one test to the next. Ideally, the zero readings of the horizontal forces should be repeatable, for a given tire type, since we follow the same procedures each time we calibrate the vehicle. This variability, however, could not be eliminated even when a marked location on the tire was rolled to the same location on a flat concrete surface and resting on the same spot on the tire circumference (with vehicle weight and temperature held constant). In retrospect, these inconsistent zero horizontal load readings are believed to be caused by slight changes in the position of the tire and suspension system (slight deviation from vertical or parallel, i.e., toe-in, camber and castor) each time the vehicle rolls to a stop.

Since the horizontal force readings for zero load were not repeatable with the current calibration method, other calibration methods were developed. Three methods of vehicle calibration, termed "air," "rolling or dynamic," and "static," were analyzed. The static calibration is the original calibration method (described earlier) where the horizontal forces are zeroed while the vehicle is motionless after it had been rolled back and forth. For the rolling calibration, the horizontal forces on the load cell are read while the vehicle is rolling slowly (1 mph) on a hard level surface, and this is used as the zero value or datum. The air calibration refers to zeroing the horizontal channels while the front end of the vehicle is jacked up with the wheels in the air. After the vehicle is jacked up, the wheels are spun and the

suspension is allowed to settle. The zero value is read after the wheels have stopped.

To compare the different calibration schemes, 10 calibrations of each type (static, rolling, and air) were performed. All calibrations were performed in a random order within two hours, to reduce outside influences (primarily temperature, as calibrations were performed outdoors). Temperature on opposite sides of each load cell as well as at various places around the inside and outside of the vehicle, were recorded and thermocouples were read periodically throughout the experiment. The entire test sequence was duplicated by other personnel the following day. The calibration values obtained for each of the tests are presented in Appendix B.

The zero readings for all calibrations are listed in Tables 5 and 6. Table 5 contains the data taken on 18 October, separated by calibration type (air, rolling and static), and similarly Table 6 summarizes the zero readings from 19 October. All values listed are digital output from the data acquisition equipment, not scaled into force units. (Scaling factors are not affected by the zero values, and they are included in the compilation of the calibrations in Appendix B.) The average, standard deviation and range are computed for the zero values of each channel for each calibration type. The time of each test and the thermocouple readings on the load cells are also listed.

The precision of the calibration methods can be evaluated by comparing the standard deviation of the zero readings for each calibration method. The standard deviations for each channel are plotted on the bar charts shown in Figures 6 (18 October) and 7 (19 October). The following generalizations can be made from these graphs:

1. In nearly all cases, the rolling calibrations are more consistent than the other calibrations (the standard deviation is lower).
2. The side channels on each load cell (LS and RS) have the highest standard deviations.
3. The air calibration was noticeably worse on 18 October than on 19 October.
4. On 19 October the calibration of the velocity sensors (Lvel, Rvel, SONIC, 5th) varied significantly more than on 18 October.

Each of these observations is addressed individually below.

1. For nearly all cases, the rolling calibration yields the best repeatability (has the smallest standard deviation). It is more consistent from test to test because the running gear is moving and thus averages any position-oriented bias suspected of being the cause of error in a static calibration. As it is essentially a hard surface resistance test, this type of calibration is not suitable if a measure of total motion resistance is desired. How-

Table 5. Zero values for each channel from the instrumented vehicle for the series of calibration tests taken on October 18, 1989.

Tables and associated statistics are separated by the type of calibration method used. All values are in counts of the data acquisition hardware (not yet converted to force or velocity units) and temperature readings are in degrees Celsius.

| No | L | | | | R | | | | Sonic Devc | Sih Wheel | Time | Thermocouples (°C) | | | |
|----------------------------|---------|--------|---------|-------|---------|--------|---------|-------|------------|-----------|------|--------------------|-------|-------|-------|
| | Ver | Long | Side | Veloc | Ver | Long | Side | Veloc | | | | 1 | 2 | 3 | 4 |
| Air Calibration | | | | | | | | | | | | | | | |
| A | -941.2 | -51.5 | -437.3 | 9.1 | -686.7 | -27.3 | -377.4 | 17.0 | 9.7 | 8.3 | 1019 | 17.2 | 13.5 | 12.7 | 10.7 |
| D | -944.5 | -49.6 | -445.1 | 10.0 | -701.8 | -26.2 | -380.0 | 17.5 | 10.3 | 8.8 | 1058 | 17.6 | 15.5 | 15.6 | 14.2 |
| H | -943.7 | -51.4 | -447.6 | 10.2 | -703.6 | -30.1 | -380.9 | 17.8 | 10.3 | 9.9 | 1124 | 20.4 | 16.8 | 16.8 | 16.3 |
| I | -944.3 | -52.6 | -448.9 | 10.1 | -702.7 | -29.1 | -379.9 | 17.9 | 10.8 | 10.0 | 1127 | 19.6 | 16.2 | 16.9 | 15.2 |
| N | -943.4 | -53.0 | -453.4 | 9.5 | -709.3 | -30.6 | -381.4 | 18.1 | 11.3 | 10.3 | 1214 | 24.2 | 20.5 | 31.7 | 21.7 |
| S | -943.1 | -3.1 | -452.9 | 10.3 | -707.5 | -31.9 | -380.9 | 18.7 | 11.1 | 9.8 | 1238 | 22.3 | 18.1 | 20.1 | 19.5 |
| T | -944.3 | -34.0 | -396.1 | 10.6 | -706.8 | -35.5 | -358.2 | 18.8 | 11.4 | 10.0 | 1248 | 24.4 | 20.6 | 19.0 | 18.9 |
| Avg | -943.50 | -49.31 | -440.19 | 9.97 | -702.63 | -30.01 | -376.96 | 17.97 | 10.77 | 9.57 | | 20.81 | 17.31 | 18.97 | 16.79 |
| Std | 1.1 | 6.4 | 18.7 | 0.5 | 7.0 | 2.9 | 7.8 | 0.6 | 0.6 | 0.7 | | 2.7 | 2.4 | 5.6 | 3.4 |
| Min | -944.5 | -53.1 | -453.4 | 9.5 | -709.3 | -35.5 | -381.4 | 17.5 | 10.3 | 8.8 | | 17.6 | 15.5 | 15.6 | 14.2 |
| Max | -943.1 | -34.0 | -396.1 | 10.6 | -701.8 | -26.2 | -358.2 | 18.8 | 11.4 | 10.3 | | 24.4 | 20.6 | 31.7 | 21.7 |
| Rolling Calibration | | | | | | | | | | | | | | | |
| C | -945.4 | -55.8 | -405.7 | 64.5 | -700.8 | 24.8 | -351.3 | 70.9 | 11.0 | 62.6 | 1043 | 19.3 | 16.9 | 13.2 | 10.1 |
| E | -942.8 | -59.6 | -401.1 | 64.1 | -698.8 | 22.0 | -343.8 | 72.6 | 10.8 | 63.7 | 1105 | 19.5 | 16.7 | 16.9 | 15.0 |
| F | -942.9 | -59.6 | -401.1 | 64.1 | -698.8 | 22.0 | -343.8 | 72.6 | 10.9 | 65.6 | 1113 | 22.9 | 19.3 | 16.0 | 16.1 |
| G | -942.9 | -61.5 | -402.5 | 63.3 | -702.2 | 20.5 | -351.9 | 73.1 | 11.2 | 64.2 | 1117 | 20.1 | 17.1 | 17.7 | 16.0 |
| K | -943.6 | -60.1 | -409.6 | 64.9 | -703.6 | 18.5 | -336.8 | 73.7 | 11.0 | 65.6 | 1136 | 20.4 | 16.9 | 17.2 | 16.2 |
| L | -942.5 | -58.8 | -407.9 | 63.0 | -702.3 | 19.8 | -343.8 | 73.0 | 11.3 | 64.2 | 1141 | 21.7 | 18.6 | 16.5 | 16.4 |
| O | -943.6 | -58.0 | -405.5 | 63.8 | -710.7 | 19.9 | -345.0 | 71.4 | 11.2 | 63.1 | 1218 | 25.7 | 21.0 | 20.4 | 20.7 |
| Avg | -943.37 | -59.06 | -404.91 | 64.00 | -702.46 | 21.07 | -345.20 | 72.47 | 11.96 | 64.14 | | 21.37 | 18.07 | 16.84 | 15.79 |
| Std | 0.9 | 1.7 | 3.1 | 0.5 | 3.8 | 1.9 | 4.8 | 0.9 | 0.2 | 1.1 | | 2.1 | 1.5 | 2.0 | 2.9 |
| Min | -945.4 | -61.5 | -409.6 | 63.3 | -710.7 | 18.5 | -351.9 | 70.9 | 10.8 | 62.6 | | 19.3 | 16.7 | 13.2 | 10.1 |
| Max | -942.5 | -55.8 | -401.1 | 64.9 | -698.8 | 24.8 | -336.8 | 73.7 | 11.3 | 65.6 | | 25.7 | 21.0 | 20.4 | 20.7 |
| Static Calibration | | | | | | | | | | | | | | | |
| B | -939.9 | -41.8 | -402.5 | 9.8 | -690.6 | 27.8 | -355.6 | 17.9 | 10.1 | 9.1 | 1033 | 20.6 | 19.2 | 15.5 | 13.2 |
| J | -944.2 | -45.2 | -413.9 | 10.0 | -702.3 | 27.5 | -369.3 | 18.2 | 11.0 | 10.4 | 1131 | 19.5 | 18.5 | 16.3 | 16.6 |
| M | -942.8 | -45.0 | -428.9 | 10.3 | -702.8 | 45.9 | -380.3 | 18.3 | 11.3 | 9.9 | 1146 | 21.9 | 17.9 | 16.8 | 16.0 |
| P | -942.4 | -40.6 | -459.7 | 9.8 | -710.4 | 46.2 | -409.0 | 17.9 | 10.9 | 10.0 | 1223 | 22.9 | 19.1 | 20.8 | 20.5 |
| Q | -944.3 | -46.2 | -426.6 | 10.3 | -708.9 | 37.6 | -385.1 | 18.3 | 11.2 | 10.1 | 1227 | 23.4 | 20.0 | 20.1 | 19.5 |
| R | -943.5 | -44.0 | -461.5 | 10.9 | -708.5 | 45.5 | -411.4 | 18.4 | 11.2 | 9.9 | 1234 | 22.3 | 18.2 | 20.7 | 20.0 |
| T | -944.3 | -34.0 | -396.1 | 10.6 | -706.8 | 35.5 | -358.2 | 18.3 | 11.4 | 10.0 | 1242 | 23.5 | 19.4 | 19.6 | 19.5 |
| Avg | -943.05 | -42.39 | -427.03 | 10.24 | -704.32 | 38.01 | -381.27 | 18.26 | 11.01 | 9.91 | | 22.01 | 18.90 | 18.54 | 17.90 |
| Std | 1.5 | 3.9 | 23.9 | 0.4 | 6.3 | 7.6 | 20.8 | 0.3 | 0.4 | 0.4 | | 1.4 | 0.7 | 2.1 | 2.5 |
| Min | -944.3 | -46.2 | -461.5 | 9.8 | -710.4 | 27.6 | -411.4 | 17.9 | 10.1 | 9.1 | | 19.5 | 17.9 | 15.5 | 13.2 |
| Max | -939.9 | -34.0 | -396.1 | 10.9 | -690.6 | 46.2 | -355.6 | 18.8 | 11.4 | 10.4 | | 23.5 | 20.0 | 20.8 | 20.5 |

Table 6. Zero values for each channel from the instrumented vehicle for the series of calibration tests taken on October 19, 1989.
 Tables and associated statistics are separated by the type of calibration method used. All values are in counts of the data acquisition hardware (not yet converted to force or velocity units) and temperature readings are in degrees Celsius.

| No. | L | | | | R | | | | Sth Wheel | Time | Thermocouples (°C) | | | | Air temp. 0 |
|----------------------------|---------|--------|---------|-------|---------|--------|---------|-------|--------------|-------|--------------------|-------|-------|-------|----------------|
| | Ver | Long | Side | Veloc | Ver | Long | Side | Veloc | | | R Devc | 1 | 2 | 3 | |
| Air Calibration | | | | | | | | | | | | | | | |
| A | -949.8 | -64.4 | -439.0 | -6.2 | -687.3 | -40.3 | -371.2 | 1.6 | -5.1 | -6.2 | 1015 | 5.7 | 5.7 | 5.7 | 8.8 |
| C | -944.5 | -55.7 | -435.9 | -0.8 | -686.7 | -33.6 | -374.2 | 7.4 | 0.3 | -1.3 | 1030 | 16.9 | 13.8 | 10.9 | 15.7 |
| F | -945.0 | -55.0 | -441.9 | 6.6 | -691.6 | -30.7 | -380.2 | 14.5 | 6.9 | 5.3 | 1104 | 21.1 | 17.8 | 14.5 | 16.4 |
| M | -946.7 | -54.0 | -452.5 | 8.0 | -695.8 | -30.8 | -381.9 | 15.8 | 8.5 | 7.1 | 1136 | 23.5 | 19.8 | 17.4 | 20.1 |
| D | -945.4 | -53.5 | -452.3 | 7.8 | -696.1 | -30.6 | -382.1 | 15.8 | 8.3 | 7.2 | 1142 | 26.5 | 21.8 | 16.9 | 17.4 |
| S | -944.7 | -55.6 | -455.7 | 8.0 | -695.1 | -28.7 | -380.7 | 16.0 | 9.0 | 7.2 | 1159 | 22.6 | 19.9 | 19.3 | 13.8 |
| V | -944.5 | -54.8 | -454.1 | 7.0 | -696.4 | -29.0 | -382.0 | 15.2 | 7.8 | 6.7 | 1211 | 22.0 | 19.2 | 18.8 | 16.2 |
| Ave | -945.80 | -56.14 | -447.34 | 4.34 | -692.71 | -31.96 | -378.90 | 12.33 | 5.09 | 3.72 | | 19.76 | 16.79 | 14.79 | 14.39 |
| Std | 1.8 | 3.5 | 7.5 | 5.2 | 3.9 | 3.7 | 4.1 | 5.2 | 5.0 | 5.0 | | 6.3 | 5.3 | 4.6 | 4.4 |
| Min | -946.7 | -55.7 | -455.7 | -0.8 | -696.4 | -33.6 | -382.1 | 7.4 | 0.3 | -1.3 | | 16.9 | 13.8 | 10.9 | 10.4 |
| Max | -944.5 | 53.5 | -435.9 | 8.0 | -686.7 | -28.7 | -374.2 | 16.0 | 9.0 | 7.2 | | 26.5 | 21.8 | 19.3 | 18.5 |
| Rolling Calibration | | | | | | | | | | | | | | | |
| G | -942.9 | -57.2 | -399.0 | 57.7 | -689.4 | 18.2 | -347.5 | 66.0 | 5.7 | 57.2 | 1056 | 20.9 | 17.3 | 13.5 | 13.2 |
| H | -945.0 | -59.4 | -403.7 | 58.9 | -689.5 | 15.8 | -340.7 | 67.2 | 6.5 | 57.7 | 1059 | 20.2 | 16.6 | 13.5 | 13.4 |
| K | -944.1 | -59.5 | -400.6 | 62.3 | -691.3 | 19.6 | -345.3 | 68.5 | 7.8 | 59.8 | 1113 | 23.3 | 19.0 | 15.3 | 15.0 |
| P | -944.0 | -53.5 | -412.5 | 59.1 | -695.0 | 14.0 | -338.8 | 67.0 | 8.8 | 58.1 | 1145 | 25.0 | 21.1 | 18.0 | 17.3 |
| Q | -943.9 | -58.6 | -399.3 | 67.7 | -696.0 | 18.5 | -348.7 | 75.5 | 8.7 | 67.6 | 1150 | 25.3 | 21.0 | 17.6 | 20.7 |
| R | -944.6 | -62.1 | -411.7 | 62.4 | -695.8 | 21.3 | -351.8 | 70.5 | 9.0 | 61.6 | 1155 | 23.2 | 19.3 | 17.5 | 16.9 |
| T | -944.8 | -60.1 | -404.1 | 57.6 | -696.6 | 22.0 | -353.5 | 66.2 | 9.1 | 58.2 | 1203 | 21.6 | 18.2 | 18.5 | 18.0 |
| Ave | -944.19 | -58.63 | -404.41 | 60.81 | -693.37 | 18.49 | -346.61 | 68.70 | 7.94 | 60.03 | | 22.79 | 18.93 | 16.27 | 15.91 |
| Std | 0.7 | 2.5 | 5.2 | 3.4 | 3.0 | 2.6 | 5.0 | 3.1 | 1.3 | 3.4 | | 1.8 | 1.6 | 2.0 | 1.9 |
| Min | -945.0 | -62.1 | -412.5 | 57.6 | -696.6 | 14.0 | -353.5 | 66.0 | 5.7 | 57.2 | | 20.2 | 16.6 | 13.5 | 13.2 |
| Max | -942.9 | -53.5 | -399.0 | 67.7 | -689.4 | 22.0 | -338.8 | 75.5 | 9.1 | 67.6 | | 25.3 | 21.1 | 18.5 | 18.0 |
| Static Calibration | | | | | | | | | | | | | | | |
| B | -946.5 | -52.0 | -393.5 | -4.3 | -686.4 | 18.0 | -369.7 | 3.1 | -3.3 | -4.8 | 1022 | 10.3 | 9.4 | 8.3 | 8.0 |
| D | -942.6 | -37.9 | -399.0 | 1.3 | -686.6 | 35.4 | -371.8 | 10.0 | 2.6 | 1.1 | 1038 | 18.3 | 14.6 | 10.7 | 10.9 |
| E | -943.8 | -43.5 | -416.3 | 3.0 | -688.0 | 28.7 | -377.4 | 11.0 | 4.2 | 2.6 | 1042 | 19.2 | 15.7 | 12.0 | 11.7 |
| F | -944.2 | -47.0 | -384.0 | 4.3 | -689.8 | 28.9 | -353.4 | 12.3 | 5.3 | 3.5 | 1049 | 20.1 | 17.0 | 13.3 | 13.2 |
| J | -945.6 | -42.4 | -474.8 | 7.3 | -692.3 | 22.4 | -420.8 | 14.9 | 7.4 | 6.0 | 1110 | 21.5 | 17.7 | 14.6 | 14.4 |
| L | -944.1 | -36.0 | -450.8 | 7.8 | -692.4 | 39.5 | -401.9 | 15.4 | 8.2 | 6.8 | 1118 | 21.8 | 18.0 | 15.2 | 17.6 |
| U | -943.6 | -42.8 | -420.9 | 7.3 | -695.4 | 25.2 | -370.2 | 14.8 | 8.2 | 6.7 | 1206 | 21.1 | 18.3 | 18.5 | 17.4 |
| Ave | -944.34 | -43.09 | -419.90 | 3.81 | -690.13 | 28.30 | -380.74 | 11.64 | 4.66 | 3.13 | | 18.90 | 15.81 | 13.27 | 13.97 |
| Std | 1.2 | 5.0 | 30.2 | 4.0 | 3.1 | 6.8 | 21.1 | 4.0 | 3.8 | 3.8 | | 3.7 | 2.9 | 3.1 | 2.9 |
| Min | -946.5 | -52.0 | -474.8 | -4.3 | -695.4 | 18.0 | -420.8 | 3.1 | -3.3 | -4.8 | | 10.3 | 9.4 | 8.3 | 8.0 |
| Max | -942.6 | -36.0 | -384.0 | 7.8 | -686.4 | 39.5 | -353.4 | 15.4 | 8.2 | 6.8 | | 21.8 | 18.3 | 18.5 | 17.4 |

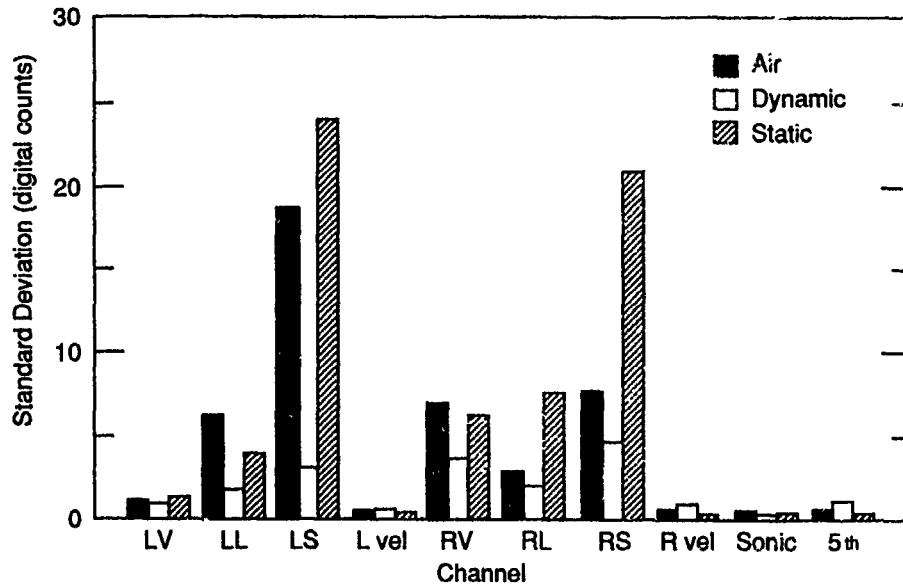


Figure 6. Bar graph comparing the standard deviations of the zero values for each channel, obtained using the three calibration methods. Data were collected on 18 October 1990.

ever, much of our research work is concerned with the resistance due to terrain deformation, and hard surface motion resistance is subtracted. For our application, then, the rolling calibration method is more consistent than static calibration and should be used when comparing the results of different terrain conditions.

2. The side channels of the load cell consistently

have the highest standard deviation. This may indicate that the side channels are more sensitive to any changes in the system (such as temperature) or that none of these calibration methods adequately zero the side load. The variability is most likely caused by the difference in the way the tire sits (slight variations in vertical or parallel) each time the vehicle rolls to a stop. Currently, the

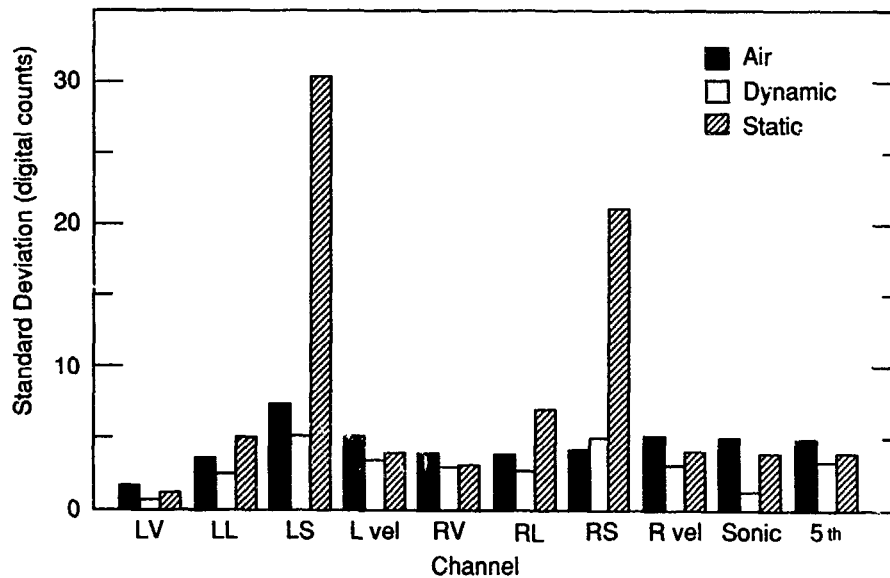


Figure 7. Bar graph comparing the standard deviations of the zero values for each channel, obtained using the three calibration methods. Data were collected on 19 October 1990.

THERMOCOUPLE LOCATIONS

1. Rear side of left wheel load cell
2. Front side of left wheel load cell
3. Rear side of right wheel load cell
4. Front side of right wheel load cell
5. Outside of right front fender
6. Outside of left front fender
7. Inside vehicle, on top of data acquisition system
8. Inside vehicle, inside data acquisition system
9. Inside rear of vehicle
0. Ambient outside temperature (mounted on mirror)

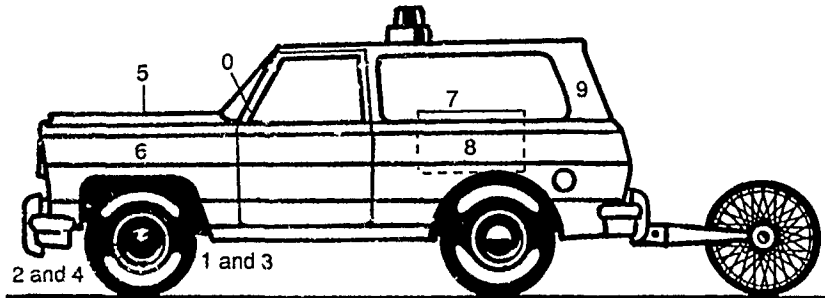


Figure 8. Location of the thermocouples on the instrumented vehicle.

information from these channels is not used in CRREL's research program but if these measurements are used in the future, a rolling or air calibration is suggested.

3. The variability in the air calibration method was surprising but is most likely due to the change in air circulation when the front of the vehicle is raised. Theoretically, the calibration in the air should be the most consistent, since the weight on the load cell is due to the wheel only and is not affected by weight distribution in the vehicle when in this position. In reality, however, the load cells are sensitive to temperature, and when the vehicle is jacked up the load cells are exposed to greater air circulation and wind action. During normal vehicle operation, the air from around the engine warms the load cells. When the front end is jacked up, the air flow is disturbed and the temperature at the load cells changes. The effects of temperature are studied more closely in the next section.

4. The last item of discussion regards the increase in the standard deviations on 19 October as compared to 18 October. Particularly striking (Fig. 6 and 7) is the large increase in the standard deviation of the velocity channels even though the vehicle was motionless during the zero readings of the velocity channels for the static and air calibrations. Again, the reason for this is likely to be changing temperature. On 18 October the vehicle was running for at least one hour before the testing began. On 19 October, the vehicle was on for only 15 minutes before testing began. It is possible that temperature at the electronics inside the vehicle or at the load cells on the vehicle's wheels had not yet stabilized on the 19th. This can also be seen in the data in Table 6. The effects of temperature are more thoroughly discussed below.

Temperature

Although the load cells on the CIV are temperature compensating, this compensation is not designed to cover the wide temperature ranges to which the load cells are subjected during cold regions mobility testing. This does not mean that the load cells are not suitable for testing in this environment, but rather that they must be closely monitored and should be calibrated at the temperature of the test and rechecked often if the test environment is changing. From experiments performed to evaluate the sensitivity of the load cells and the cause of the scatter in the data, we have collected information regarding their behavior during temperature changes.

The sensitivity of the load cells to temperature was first tested in the laboratory by applying heat to the load cell with a heat gun while reading the load cell output. The heat gun caused both a bulk temperature change as well as a temperature gradient across the load cell. The load cell output changed rapidly as the heat was applied and removed. Because of the large effect of temperature, the vehicle and load cells and other parts of the vehicle were instrumented with thermocouples for a more thorough study. Two thermocouples were placed on each load cell, one in front and one to the rear, to monitor the temperature difference across the cell. Six additional thermocouples were placed throughout the vehicle as indicated in Figure 8.

The data obtained during the calibration schemes discussed earlier were analyzed for the effect of temperature. Figures 9 and 10 show the ambient air and load cell temperature as a function of time for the test series on 18 and 19 October, respectively. Both figures show a drift in temperature with time. Since the load cells located at the wheel axle are sensitive to temperature,

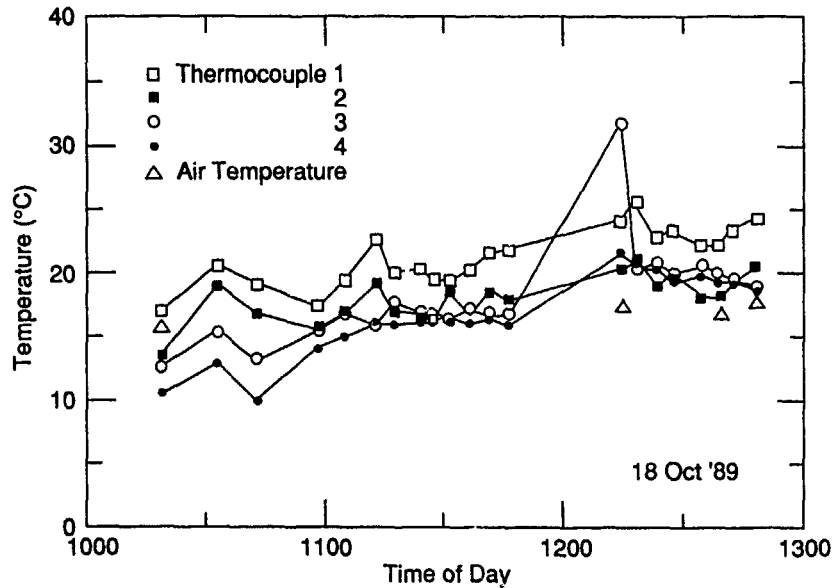


Figure 9. Temperatures measured at the load cells and the ambient temperature measured on 18 October .

the temperature around the instrumentation both inside and outside of the vehicle must stabilize before calibrating and testing. The heat from the engine circulates around the wheels and it takes some time after the engine is turned on before the temperature of the engine, vehicle, load cells and velocity sensors stabilizes. From Figure 10 it appears that on 19 October, the air temperature was rising and the temperature at the load cells had not stabilized before the testing began. This probably

caused the additional scatter in the calibration data on 19 October. Figure 10 indicates that an additional 20 to 30 minutes is necessary for the temperatures to stabilize. The data in Table 6 agree with this and show that the anomalous velocity readings occur within the first 30 to 45 minutes of testing. Obviously, this is a function of the initial temperature of the vehicle and the outside air temperature but, as a rule of thumb, the vehicle should "soak" in the test environment with all equip-

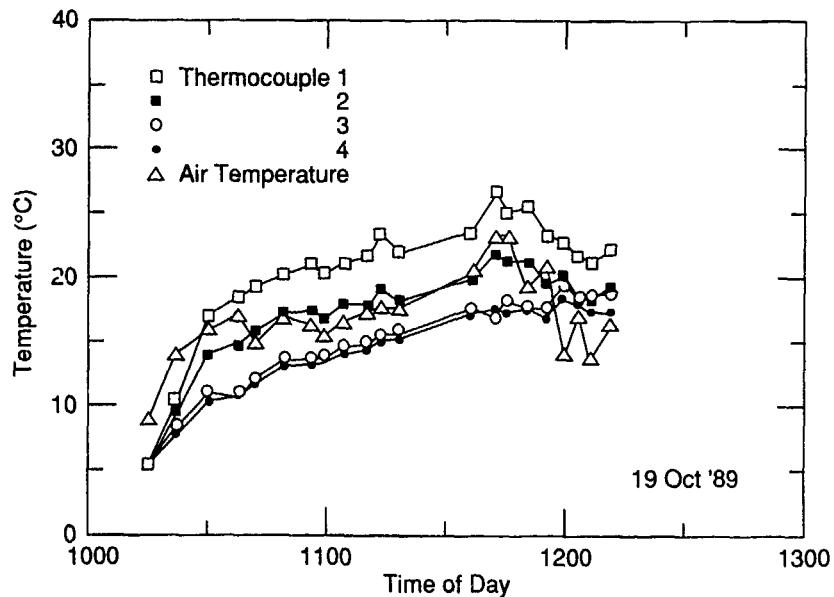


Figure 10. Temperatures measured at the load cells and the ambient temperature measured on October 19.

ment and electronics turned on. (Since the new load cells for the vehicle have a steel casing that has a lower thermal diffusivity than the current load cell casing of aluminum, the new load cells may have to soak longer but should be more stable since they respond to temperature more slowly.)

The zero values for each wheel were plotted against the average temperature at each of the load cells to evaluate how the temperature influences the load cell reading. One such plot showing a strong correlation between the zero values (corrected by subtracting the average value of that channel) and the average of the temperatures taken at that wheel is shown in Figure 11. This plot is based on the data from the series of air calibrations performed on 19 October. The change in load cell readings reflects a change on the order of 10 lbf. Although Figure 11 shows that the load cell and velocity zero value is changing with temperature, it does not prove that the change in temperature at the wheel is responsible. This could be a case of correlation

but not causation. It is particularly odd that the zero of the velocity channel is sensitive to temperature. Since the velocity sensors are proximity gauges that are not generally affected by temperature, the temperature sensitivity must be elsewhere in the system. The amplifiers in the velocity signal conditioning unit are the most likely cause. Although the electronics in the data acquisition system technically need no warm up time, they are sensitive to temperature and are designed to operate at a constant temperature, generally at room temperature. Therefore, the temperature inside the vehicle (with all electronics on) must stabilize before testing. The electronics in the vehicle actually produce quite a bit a heat themselves, particularly the computer, and must be cooled using fans. From the calibration tests, I have been unable to distinguish whether the temperature at the wheels or the temperature at the electronics, or both, is affecting the readings since the temperature inside the vehicle was not monitored during this set of tests.

The temperatures both at the load cells and at the data

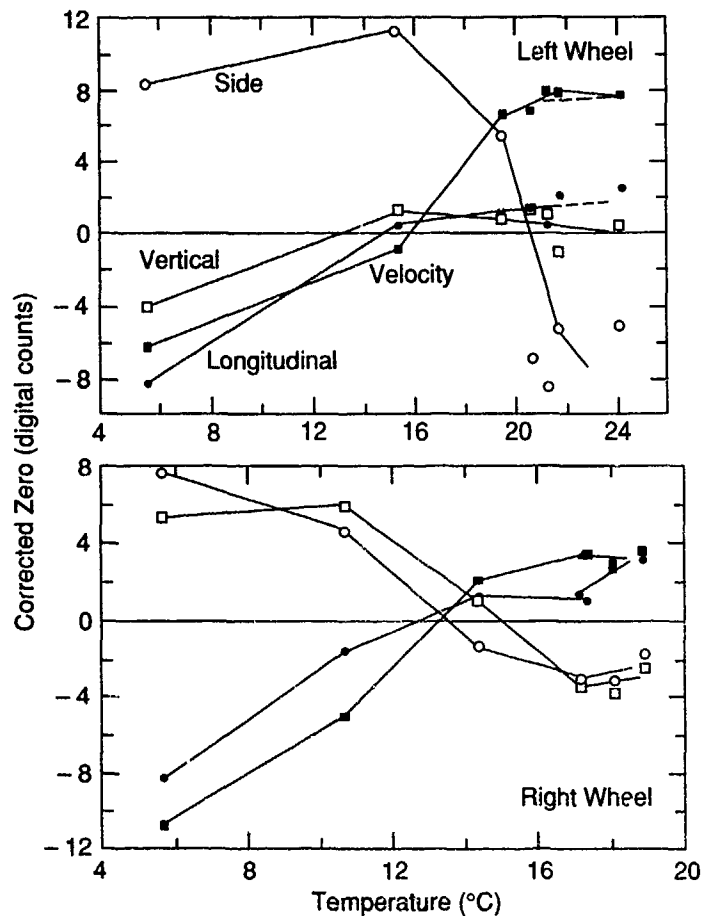


Figure 11. Load cell and velocity zero readings vs average temperature at the load cell.

acquisition system inside the vehicle were monitored during the experiments designed to evaluate the effect of speed (discussed later), and these data were also analyzed to determine the effect of temperature on our load cell readings. For these experiments, hard surface rolling resistance tests were performed five times each at six different vehicle speeds, in random order. The entire sequence was performed three times for different tire inflation pressures and calibration methods. The longitudinal force measured by the load cells, the temperature recorded at the load cells (thermocouples 1-4),

the ambient outside air temperature (thermocouple number 0), the temperature at the data acquisition system (thermocouple number 8) are given in Tables 7, 8 and 9. The longitudinal force (hard surface rolling resistance) was compared to the average temperature of each load cell, the temperature differential across each load cell and the temperature at the data acquisition hardware inside the vehicle. To eliminate the effect of speed, the temperature effect was studied separately at each speed.

The analysis of this data set for temperature effects

Table 7. Results of rolling resistance measured at different speeds.

Data were taken with tires inflated to 26 psi, using a static calibration. Time of the test and the temperature at each of the load cells were also recorded.

| Test | Speed (mph) | Rolling resistance | | Time | Air temp. (°C) | Thermocouple | | Left wheel | | Thermocouple | | Right wheel | | Thermocouple 8 (°C) |
|----------|-------------|--------------------|-------------|------|----------------|--------------|--------|------------|-----------------|--------------|--------|-------------|-----------------|---------------------|
| | | Left (lbf) | Right (lbf) | | | 1 (°C) | 2 (°C) | Avg. (°C) | Difference (°C) | 3 (°C) | 4 (°C) | Avg. (°C) | Difference (°C) | |
| 1101D | 1 | 10.2 | 1.7 | 1007 | 20.0 | 18.2 | 19.7 | 19.0 | -1.5 | 18.2 | 16.5 | 17.4 | 1.7 | 28.6 |
| 1101J | 1 | 7.6 | 7.5 | 1030 | 15.5 | 14.2 | 13.9 | 14.1 | 0.3 | 14.4 | 14.2 | 14.3 | 0.2 | 25.0 |
| 1101L | 1 | 9.0 | 4.0 | 1034 | 15.8 | 14.2 | 14.7 | 14.4 | -0.5 | 14.3 | 14.2 | 14.3 | 0.1 | 25.0 |
| 1101U | 1 | 5.8 | 4.2 | 1229 | 18.0 | 17.1 | 19.3 | 18.2 | -2.2 | 18.5 | 16.6 | 17.6 | 1.9 | 28.3 |
| 1101V | 1 | 8.6 | 2.0 | 1230 | 17.5 | 17.7 | 18.9 | 18.3 | -1.2 | 18.2 | 16.3 | 17.3 | 1.9 | 28.3 |
| Average: | | 8.24 | 3.88 | | | | | | | | | | | |
| Std: | | 1.7 | 2.3 | | | | | | | | | | | |
| 1101E | 3 | 8.7 | 2.8 | 1011 | 23.0 | 19.4 | 19.9 | 19.6 | -0.5 | 17.9 | 18.5 | 18.2 | -0.6 | 26.0 |
| 1101R | 3 | 7.9 | 4.2 | 1220 | 21.0 | 19.2 | 23.0 | 21.1 | -3.8 | 22.1 | 19.9 | 21.0 | 2.2 | 28.1 |
| 1101S | 3 | 7.4 | 6.4 | 1223 | 19.0 | 17.9 | 21.7 | 19.8 | -3.8 | 20.4 | 17.9 | 19.2 | 2.5 | 28.2 |
| 1101X | 3 | 9.6 | 4.9 | 1233 | 16.5 | 18.6 | 18.0 | 18.3 | 0.7 | 17.7 | 17.6 | 17.7 | 0.1 | 28.4 |
| 1101— | 3 | 7.9 | 5.9 | 1244 | 18.4 | 16.7 | 18.7 | 17.7 | -2.0 | 17.9 | 18.8 | 18.4 | -0.9 | 28.8 |
| Average: | | 8.3 | 4.84 | | | | | | | | | | | |
| Std: | | 0.7 | 1.4 | | | | | | | | | | | |
| 1101C | 5 | 10.5 | 6.6 | 1001 | 17.6 | 16.2 | 19.6 | 17.9 | -3.4 | 18.5 | 12.3 | 15.4 | 6.2 | 32.8 |
| 1101H | 5 | 7.0 | 7.1 | 1025 | 17.7 | 15.6 | 15.7 | 15.7 | -0.1 | 14.5 | 14.5 | 14.5 | 0.0 | 24.7 |
| 1101M | 5 | 6.9 | 5.8 | 1035 | 16.0 | 14.1 | 15.0 | 14.6 | -0.9 | 14.3 | 14.2 | 14.3 | 0.1 | 25.0 |
| 1101I | 5 | 8.5 | 5.4 | 1238 | 16.9 | 18.1 | 18.0 | 18.0 | 0.2 | 17.6 | 18.4 | 18.0 | -0.8 | 28.6 |
| 1101N | 5 | 6.5 | 4.9 | 1239 | 17.3 | 17.8 | 18.1 | 18.0 | -0.3 | 17.7 | 18.5 | 18.1 | -0.8 | 28.7 |
| Average: | | 7.88 | 5.96 | | | | | | | | | | | |
| Std: | | 1.7 | 0.9 | | | | | | | | | | | |
| 1101A | 10 | 10.0 | 6.8 | 910 | — | — | — | — | — | — | — | — | — | — |
| 1101B | 10 | 10.3 | 7.7 | 952 | — | — | — | — | — | — | — | — | — | — |
| 1101K | 10 | 8.8 | 9.2 | 1032 | 15.7 | 14.2 | 14.3 | 14.2 | -0.1 | 14.4 | 14.2 | 14.3 | 0.2 | 25.0 |
| 1101W | 10 | 7.2 | 8.2 | 1232 | 17.0 | 18.2 | 18.5 | 18.4 | -0.3 | 17.9 | 17.0 | 17.5 | 0.9 | 28.4 |
| 1101Y | 10 | 7.9 | 8.9 | 1234 | 16.1 | 18.9 | 17.7 | 18.3 | 1.2 | 17.5 | 18.1 | 17.8 | -0.6 | 28.5 |
| Average: | | 8.84 | 8.16 | | | | | | | | | | | |
| Std: | | 1.3 | 1.0 | | | | | | | | | | | |
| 1101F | 15 | 8.3 | 5.7 | 1017 | 26.9 | 23.2 | 20.0 | 21.6 | 3.2 | 17.7 | 20.1 | 18.9 | -2.4 | 24.4 |
| 1101G | 15 | 10.9 | 9.3 | 1021 | 17.7 | 15.9 | 16.2 | 16.1 | -0.3 | 14.8 | 13.9 | 14.4 | 0.9 | 24.5 |
| 1101Z | 15 | 8.6 | 7.8 | 1237 | 16.4 | 18.5 | 17.9 | 18.2 | 0.6 | 17.6 | 18.3 | 17.9 | -0.7 | 28.5 |
| 1101J | 15 | 8.0 | 8.5 | 1240 | 17.8 | 17.5 | 18.3 | 17.9 | -0.8 | 17.8 | 18.6 | 18.2 | -0.8 | 28.7 |
| 1101A | 15 | 9.0 | 8.8 | 1242 | 18.0 | 17.1 | 18.6 | 17.8 | -1.5 | 17.9 | 18.7 | 18.3 | -0.8 | 28.8 |
| Average: | | 8.96 | 8.02 | | | | | | | | | | | |
| Std: | | 1.2 | 1.4 | | | | | | | | | | | |
| 1101I | 20 | 12.4 | 11.6 | 1028 | 16.2 | 14.7 | 14.8 | 14.8 | -0.1 | 14.5 | 14.2 | 14.4 | 0.3 | 24.9 |
| 1101N | 20 | 12.2 | 12.4 | 1038 | 16.2 | 14.1 | 15.2 | 14.7 | -1.1 | 14.2 | 14.2 | 14.2 | 0.0 | 25.2 |
| 1101O | 20 | 12.8 | 12.4 | 1041 | 14.6 | 13.5 | 14.0 | 13.8 | -0.5 | 13.4 | 12.6 | 13.0 | 0.8 | 25.3 |
| 1101Q | 20 | 8.5 | 6.8 | 1218 | 23.6 | 20.9 | 24.6 | 22.8 | -3.7 | 23.0 | 21.9 | 22.5 | 1.1 | 25.8 |
| 1101T | 20 | 9.9 | 8.2 | 1225 | 18.2 | 16.8 | 19.6 | 18.2 | -2.8 | 19.4 | 16.9 | 18.2 | 2.5 | 28.3 |
| Average: | | 11.16 | 10.28 | | | | | | | | | | | |
| Std: | | 1.9 | 2.6 | | | | | | | | | | | |

Table 8. Results of rolling resistance measured at different speeds.

Data were taken with tires inflated to 15 psi, using a rolling calibration. Time of the test and the temperature at each of the load cells were also recorded.

| Test | Speed (mph) | Rolling resistance | | Time | Air temp. (°C) | Thermocouple | | Avg. left (°C) | Thermocouple | | Right wheel | | Thermocouple 8 (°C) |
|----------|-------------|--------------------|-------------|------|----------------|--------------|--------|----------------|--------------|--------|-------------|-----------------|---------------------|
| | | Left (lbf) | Right (lbf) | | | 1 (°C) | 2 (°C) | | 3 (°C) | 4 (°C) | Avg. (°C) | Difference (°C) | |
| 1121I | 1 | -7.1 | -4.2 | 1402 | 5.1 | 2.7 | — | 2.7 | 3.6 | 2.8 | 3.2 | 0.8 | 14.2 |
| 1121M | 1 | -5.9 | -2.8 | 1410 | 4.4 | 1.9 | — | 1.9 | 2.9 | 2.3 | 2.6 | 0.6 | 15.3 |
| 1121N | 1 | -5.2 | -3.6 | 1411 | 4.0 | 1.6 | — | 1.6 | 2.7 | 2.3 | 2.5 | 0.4 | 15.5 |
| 1121W | 1 | -8.5 | -4.5 | 1426 | 3.1 | 0.9 | — | 0.9 | 2.2 | 2.7 | 2.5 | -0.5 | 16.6 |
| 1121^ | 1 | -7.2 | -1.9 | 1435 | -2.0 | 1.0 | — | 1.0 | 0.5 | 0.6 | 0.6 | -0.1 | 8.3 |
| Average: | | -6.78 | -3.40 | | | | | | | | | | |
| Std: | | 1.3 | 1.1 | | | | | | | | | | |
| 1121K | 3 | -4.2 | -1.8 | 1406 | 5.1 | 2.5 | — | 2.5 | 3.3 | 2.2 | 2.8 | 1.1 | 14.8 |
| 1121P | 3 | -6.9 | -4.0 | 1413 | 3.3 | 1.1 | — | 1.1 | 2.3 | 2.4 | 2.4 | -0.1 | 16.0 |
| 1121Z | 3 | -6.2 | -2.4 | 1430 | 3.5 | 0.8 | — | 0.9 | 0.9 | 2.8 | 1.8 | -2.0 | 12.1 |
| 1121] | 3 | -5.6 | -2.1 | 1434 | -1.3 | 1.3 | — | 1.3 | 0.8 | 0.9 | 0.9 | -0.2 | 10.5 |
| 1121_ | 3 | 5.6 | 2.1 | 1437 | -2.8 | 0.3 | — | 0.3 | 0.3 | 0.3 | 0.3 | -0.1 | -1.3 |
| Average: | | -3.46 | -1.64 | | | | | | | | | | |
| Std: | | 5.2 | 2.3 | | | | | | | | | | |
| 1121G | 5 | -4.2 | -1.9 | 1358 | 5.0 | 2.9 | — | 2.9 | 3.9 | 3.3 | 3.6 | 0.5 | 13.6 |
| 1121J | 5 | -3.5 | -2.3 | 1404 | 5.1 | 2.6 | — | 2.6 | 3.4 | 2.5 | 3.0 | 1.0 | 14.5 |
| 1121L | 5 | -4.1 | 0.0 | 1408 | 4.7 | 2.2 | — | 2.2 | 3.1 | 2.2 | 2.7 | 0.9 | 15.0 |
| 1121O | 5 | -2.1 | -0.6 | 1412 | 3.7 | 1.4 | — | 1.4 | 2.5 | 2.4 | 2.4 | 0.1 | 15.8 |
| 1121[| 5 | -5.4 | -2.3 | 1431 | 0.2 | 1.5 | — | 1.5 | 1.3 | 1.6 | 1.4 | -0.3 | 15.0 |
| Average: | | -3.86 | -1.42 | | | | | | | | | | |
| Std: | | 1.2 | 1.1 | | | | | | | | | | |
| 1121A | 10 | -0.2 | 2.0 | 1345 | 0.4 | 2.3 | — | 2.3 | 0.0 | 0.4 | 0.2 | -0.4 | 12.2 |
| 1121S | 10 | -2.7 | -0.1 | 1418 | 2.6 | 0.5 | — | 0.5 | 1.9 | 2.5 | 2.2 | -0.6 | 16.5 |
| 1121X | 10 | -0.7 | 1.4 | 1428 | 3.2 | 1.0 | — | 1.0 | 2.3 | 2.8 | 2.6 | -0.5 | 16.6 |
| 1121' | 10 | -2.6 | -1.2 | 1438 | 2.8 | 1.6 | — | 1.6 | 0.6 | 2.5 | 1.6 | -1.9 | 17.2 |
| 1121N | 10 | 2.6 | 1.2 | 1432 | -0.5 | 1.4 | — | 1.4 | 1.0 | 1.3 | 1.1 | -0.2 | 12.7 |
| Average: | | -0.72 | 0.66 | | | | | | | | | | |
| Std: | | 2.2 | 1.3 | | | | | | | | | | |
| 1121B | 15 | 0.5 | -2.6 | 1347 | 1.6 | 2.5 | — | 2.5 | 1.0 | 1.2 | 1.1 | -0.2 | 12.5 |
| 1121F | 15 | 1.4 | -1.2 | 1355 | 5.0 | 3.0 | — | 3.0 | 4.0 | 3.6 | 3.8 | 0.4 | 13.3 |
| 1121R | 15 | -2.4 | -2.4 | 1415 | 3.0 | 0.8 | — | 0.8 | 2.1 | 2.5 | 2.3 | -0.4 | 16.3 |
| 1121V | 15 | 2.2 | -1.4 | 1424 | 3.0 | 0.8 | — | 0.8 | 2.1 | 2.7 | 2.4 | -0.5 | 16.6 |
| 1121Y | 15 | 1.5 | -1.4 | 1429 | 4.3 | 0.9 | — | 0.9 | 1.1 | 3.1 | 2.1 | -2.0 | 14.4 |
| Average: | | 0.64 | -1.8 | | | | | | | | | | |
| Std: | | 1.8 | 0.7 | | | | | | | | | | |
| 1121D | 20 | 0 | 1.1 | 1350 | 2.7 | 2.7 | — | 2.7 | 2.0 | 2.0 | 2.0 | 0.0 | 12.8 |
| 1121E | 20 | -2.2 | 2.2 | 1353 | 3.9 | 2.8 | — | 2.8 | 3.0 | 2.8 | 2.9 | 0.2 | 13.0 |
| 1121H | 20 | -0.5 | 2.6 | 1400 | 5.0 | 2.8 | — | 2.8 | 3.7 | 3.0 | 3.4 | 0.7 | 13.9 |
| 1121T | 20 | 0.7 | 4 | 1420 | 2.7 | 0.6 | — | 0.6 | 2.0 | 2.6 | 2.3 | -0.6 | 16.5 |
| 1121U | 20 | 1 | 2.7 | 1422 | 2.8 | 0.7 | — | 0.7 | 2.1 | 2.6 | 2.3 | -0.6 | 16.5 |
| Average: | | -0.20 | 2.52 | | | | | | | | | | |
| Std: | | 1.3 | 1.0 | | | | | | | | | | |

was inconclusive. The results indicate that neither the temperature difference across the load cells nor the temperature at the data acquisition system consistently affect the load cell reading. In fact, the average temperature at the load cells did not affect the measured resistance, even though temperature is known to affect rolling resistance as indicated in Figure 12 (Clark 1982). It is likely that the temperature did not vary widely enough to detect such an effect (i.e., the range of temperatures tested was too small). In any case, based on the

results of these tests, a more rigorous study, designed specifically to look at the effect of temperature on the load cells and the velocity sensors, is recommended.

Vehicle speed

While performing hard surface rolling resistance tests, my coworkers and I noticed that the resistance increased with even a slight increase in vehicle speed. Although an increase in motion resistance with speed has been documented for higher speeds, greater than 30

Table 9. Results of rolling resistance measured at different speeds.

Data were taken with tires inflated to 15 psi, using a static calibration. Time of the test and the temperature at each of the load cells were also recorded.

| Test | Speed (mph) | Rolling Resistance | | Time | Air temp. (°C) | Thermocouple | | | Thermocouple | | Right Wheel | | Thermocouple 8 (°C) |
|----------|-------------|--------------------|-------------|------|----------------|--------------|--------|----------------|--------------|--------|----------------------|-----|---------------------|
| | | Left (lbf) | Right (lbf) | | | 1 (°C) | 2 (°C) | Avg. left (°C) | 3 (°C) | 4 (°C) | Avg. Difference (°C) | | |
| 0117H | 1 | 12.9 | 32.6 | 1053 | 8.2 | 7.6 | — | 7.6 | 5.3 | 4.3 | 4.8 | 1.0 | 21.4 |
| 0117L | 1 | 14.4 | 30.2 | 1103 | 8.1 | 7.6 | — | 7.6 | 5.5 | 4.3 | 4.9 | 1.2 | 21.5 |
| 0117M | 1 | 15.2 | 31.4 | 1105 | 8.1 | 7.6 | — | 7.6 | 5.6 | 4.3 | 4.9 | 1.3 | 21.5 |
| 0117U | 1 | 13.8 | 27.4 | 1133 | 3.7 | 8.7 | — | 8.7 | 6.8 | 4.6 | 5.7 | 2.3 | 28.2 |
| 0117Λ | 1 | 14.9 | 30.3 | 1158 | 6.0 | 6.6 | — | 6.6 | 4.8 | 3.2 | 4.0 | 1.7 | 20.6 |
| Average: | | 14.24 | 30.38 | | | | | | | | | | |
| Std: | | 0.9 | 1.9 | | | | | | | | | | |
| 0117J | 3 | 19.0 | 31.6 | 1957 | 8.1 | 7.6 | — | 7.6 | 5.4 | 4.3 | 4.9 | 1.1 | 21.5 |
| 0117O | 3 | 15.0 | 28.9 | 1111 | 7.9 | 7.6 | — | 7.6 | 5.6 | 4.3 | 5.0 | 1.3 | 21.6 |
| 0117X | 3 | 13.8 | 28.3 | 1144 | 5.0 | 7.9 | — | 7.9 | 5.8 | 3.9 | 4.9 | 1.9 | 24.8 |
| 0117[| 3 | 14.7 | 27.7 | 1156 | 5.8 | 6.8 | — | 6.8 | 5.0 | 3.4 | 4.2 | 1.7 | 20.2 |
| 0117] | 3 | 14.6 | 30.1 | 1201 | 6.1 | 6.2 | — | 6.2 | 4.6 | 3.1 | 3.8 | 1.6 | 21.0 |
| Average: | | 15.42 | 29.32 | | | | | | | | | | |
| Std: | | 2.1 | 1.6 | | | | | | | | | | |
| 0117F | 5 | 12.9 | 30.6 | 1043 | 8.3 | 7.5 | — | 7.5 | 5.2 | 4.3 | 4.8 | 0.9 | 21.3 |
| 0117I | 5 | 17.2 | 32.6 | 1055 | 8.2 | 7.6 | — | 7.6 | 5.4 | 4.3 | 4.8 | 1.1 | 21.4 |
| 0117K | 5 | 14.0 | 30.9 | 1100 | 8.1 | 7.6 | — | 7.6 | 5.5 | 4.3 | 4.9 | 1.2 | 21.5 |
| 0117N | 5 | 13.3 | 32.4 | 1107 | 8.0 | 7.6 | — | 7.6 | 5.6 | 4.3 | 4.9 | 1.3 | 21.6 |
| 0117Y | 5 | 14.0 | 30.2 | 1147 | 5.3 | 7.6 | — | 7.6 | 5.2 | 3.7 | 4.5 | 1.5 | 21.9 |
| Average: | | 14.28 | 31.34 | | | | | | | | | | |
| Std: | | 1.7 | 1.1 | | | | | | | | | | |
| 0117A | 10 | 20.0 | 33.9 | 1010 | 2.3 | 8.8 | — | 8.8 | 9.2 | 7.0 | 8.1 | 2.2 | 21.0 |
| 0117Q | 10 | 13.7 | 32.7 | 1117 | 6.2 | 8.1 | — | 8.1 | 6.3 | 4.5 | 5.4 | 1.8 | 24.2 |
| 0117V | 10 | 13.6 | 31.6 | 1137 | 4.3 | 8.5 | — | 8.5 | 6.4 | 4.3 | 5.4 | 2.1 | 26.5 |
| 0117Z | 10 | 15.3 | 33.0 | 1152 | 5.6 | 7.1 | — | 7.1 | 5.1 | 3.6 | 4.3 | 1.6 | 19.8 |
| 0117^ | 10 | — | — | 1205 | 6.2 | 5.9 | — | 5.9 | 4.4 | 3.0 | 3.7 | 1.4 | 22.0 |
| Average: | | 15.65 | 32.80 | | | | | | | | | | |
| Std: | | 3.0 | 1.0 | | | | | | | | | | |
| 0117B | 15 | 20.7 | 36.8 | 1025 | 5.2 | 8.4 | — | 8.4 | 8.2 | 5.8 | 7.0 | 2.4 | 21.1 |
| 0117E | 15 | 17.2 | 35.0 | 1039 | 8.3 | 7.5 | — | 7.5 | 5.2 | 4.3 | 4.8 | 0.9 | 21.3 |
| 0117F | 15 | 16.5 | 33.9 | 1113 | 7.2 | 7.9 | — | 7.9 | 5.9 | 4.4 | 5.2 | 1.5 | 22.9 |
| 0117T | 15 | 16.5 | 34.9 | 1128 | 3.2 | 8.9 | — | 8.9 | 7.0 | 4.8 | 5.9 | 2.2 | 21.8 |
| 0117W | 15 | 15.7 | 32.5 | 1140 | 4.5 | 8.2 | — | 8.2 | 6.2 | 4.1 | 5.2 | 2.1 | 26.5 |
| Average: | | 17.32 | 34.62 | | | | | | | | | | |
| Std: | | 2.0 | 1.9 | | | | | | | | | | |
| 0117C | 20 | 20.4 | 35.8 | 1030 | 6.3 | 8.0 | — | 8.0 | 7.2 | 5.1 | 6.2 | 2.1 | 21.1 |
| 0117D | 20 | 22.9 | 36.4 | 1035 | 7.5 | 7.7 | — | 7.7 | 6.2 | 4.7 | 5.5 | 1.5 | 21.3 |
| 0117G | 20 | 20.4 | 35.5 | 1047 | 8.2 | 7.6 | — | 7.6 | 5.3 | 4.3 | 4.8 | 1.0 | 21.4 |
| 0117R | 20 | 17.0 | 34.6 | 1120 | 5.2 | 8.5 | — | 8.5 | 6.5 | 4.6 | 5.6 | 1.9 | 25.5 |
| 0117S | 20 | 16.9 | 35.3 | 1124 | 4.2 | 8.7 | — | 8.7 | 6.7 | 4.7 | 5.7 | 2.0 | 26.9 |
| Average: | | 19.52 | 35.52 | | | | | | | | | | |
| Std: | | 2.6 | 0.7 | | | | | | | | | | |

mph (Fig. 12, Clark 1982), at low speeds resistance was assumed to be constant.

To document the effect of speed on the resistance, a series of hard surface resistance tests were performed (as mentioned in the previous section) in the same location on an asphalt road. All tests were performed within two hours to limit environmental effects. Five tests were run at each speed: 1, 3, 5, 10, 15, and 20 mph, and the test order was randomized to eliminate bias. Two series of tests (Tables 7 and 9) were performed

based on the static calibration method, one at 15-psi and another at 26-psi tire inflation pressures. One other set of tests (Table 8) was performed based on the rolling calibration method (tires at 15-psi inflation pressure). Since the calibration methods varied, the resistance values obtained are relative to the calibration method but the effect of speed is consistent.

All the test results indicate an increase in resistance with speed as shown graphically in Figures 13, 14 and 15. By fitting a straight line to the data, the slope

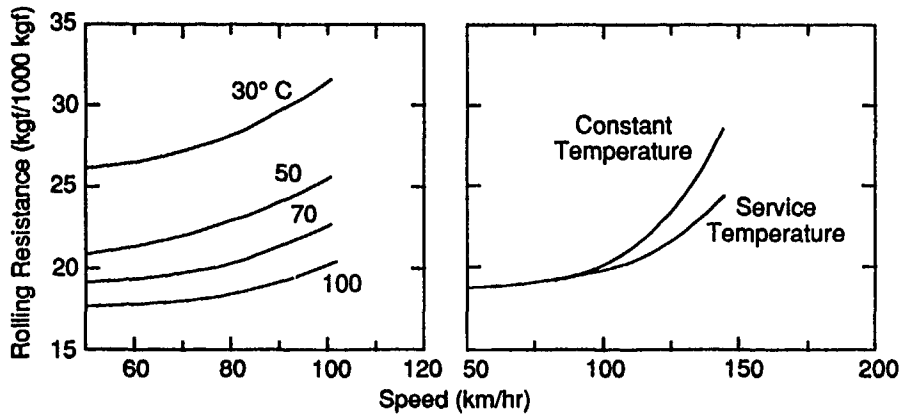


Figure 12. Rolling resistance vs speed (at high speeds, after Clark, 1982).

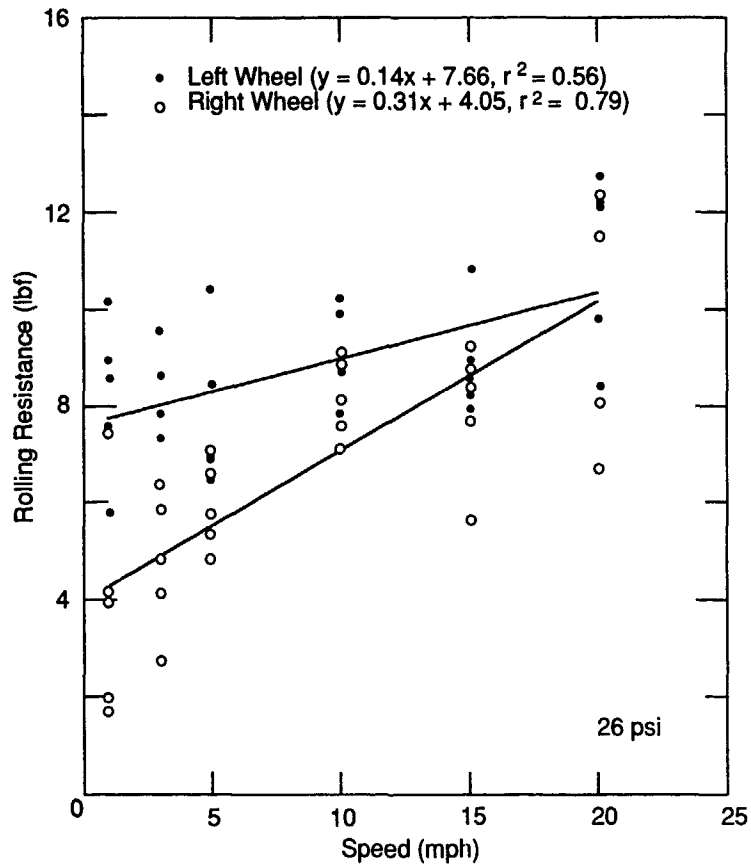


Figure 13. Hard surface motion resistance vs vehicle speed (tire pressure at 26 psi, using a static calibration method). Regression equations and correlation coefficients shown.

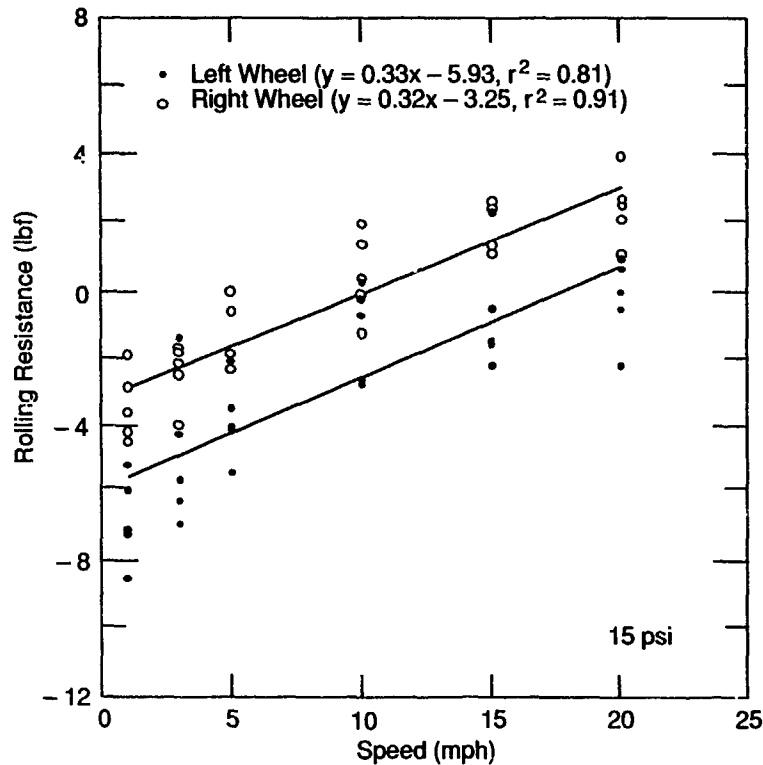


Figure 14. Hard surface motion resistance vs vehicle speed (rolling calibration, 15 psi tire inflation pressure). Regression equations and correlation coefficients are shown.

indicates the change in resistance with speed for this speed range. The straight line regression equations along with correlation coefficients are given on the figures. Slopes range from 0.14 to 0.33 lbf/mph. If the slope of 0.14 lbf/mph is omitted as an outlier, the slopes averages 0.31 lbf/mph. This is small, unless you are trying to detect very small effects .

Contact patch area

Indirectly related to uncertainty in the vehicle mobility measurements is the area of the contact patch of the tire. Static tire contact patch area is generally measured by making a print of the tire contact area on a hard surface. Because the difference between a static and rolling contact patch is small when measured on a hard surface (Clark 1982), the static, hard surface contact area is used as input to calculate the dynamic contact area on deformable terrain.

Variability in the measured contact area was noted when the same tire was measured at several different times over the course of a year. Although some of the variability may be attributed to tire wear and loosening of the sidewall bands, this should be insignificant because of the limited use of the tires. The possible effect

of the tread pattern repetition was also observed but was found to have little or no influence on the contact patch area. All measurements were taken indoors, generally in a garage area where temperatures may have been slightly different from test to test, causing some changes in the flexibility of the rubber, but again this is not believed to be the major cause of variability. In addition, although the standard tire gauge used to measure inflation pressure was calibrated, some accuracy is lost in reading the dial gauge. The primary cause of variability is believed to be changes of the normal load on the front axle caused by the load distribution in the rear of the vehicle. So, although we made no visible changes (aside from those noted on the graph), the normal load on the front axle could have changed.

Although a thorough study of the causes of variability was not performed, an indication of the magnitude of the variability and the effects of the changes of load distribution in the vehicle can be seen in Figures 16 and 17, showing contact area measured for a variety of conditions. These figures indicate the variability in the measurement as well as how the weight distribution in the vehicle affects the contact area. The figures are for the same tire at two inflation pressures, 15 psi (Fig. 16),

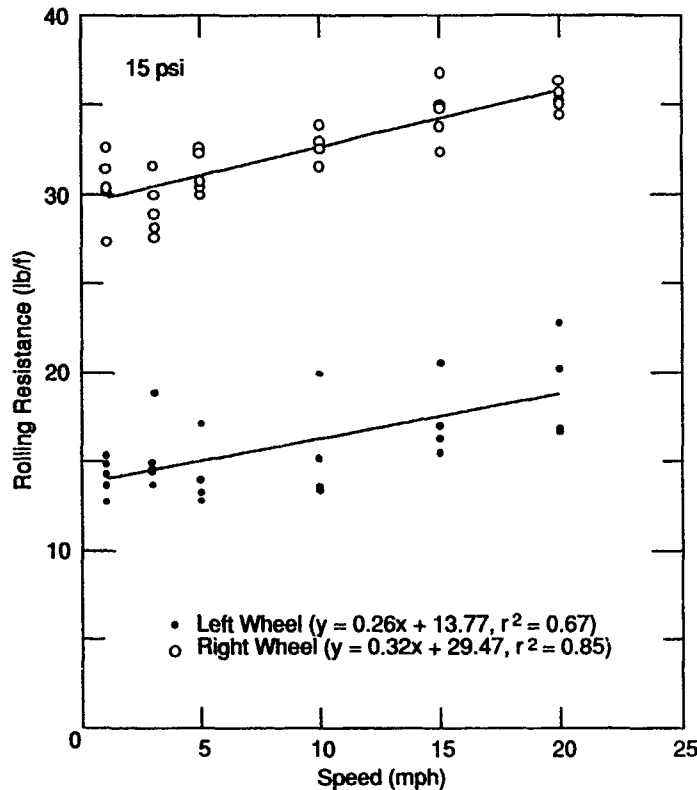


Figure 15. Hard surface motion resistance vs vehicle speed (static calibration, 26 psi tire inflation pressure). Regression equations and correlation coefficients are shown.

and 26 psi (Fig. 17). The contact area was measured with three different sets of weights on the front bumper (listed on the horizontal axis). The dates of the measurements and number of people in the vehicle are noted on the graphs. The relationship of the added weights, normal load on the wheel, deflection and contact area is shown in Table 10.

From the graphs, the effect of the weights on the front bumper is clear. However, the effect of the weight of the passengers is overshadowed by other variations in the measurement. Aside from the weights on the bumper, other variables cause the area measurements to vary by approximately 11% at 26 psi and 21% at 15 psi.

The contact area was measured at set inflation pressures and, although contact area is a function of inflation pressure, it is more directly related to tire deflection (Table 10). If inflation pressure and normal load are varied to maintain a constant tire deflection, then the contact area of the tire will remain essentially constant (Clark 1982). Therefore, in measuring contact area based on inflation pressure, care must be taken to achieve the same tire deflection. The vehicle should be

loaded the same as during testing (i.e., two persons and all equipment), and both the contact area and tire inflation pressure should be measured at the same temperature as expected during mobility testing.

Even following these guidelines and taking repeated measurements under the same conditions, some variability in the area may result from randomness associated with lowering the tire onto the paper. We know that the tire does not always roll to a stop in the same position and likewise will probably not settle in the same position when lowered using a jack. Although contact area is used in many of our mobility calculations, the uncertainty in its measurement appears to be small when compared to the variations associated with the deformable terrain.

DISCUSSION AND APPLICATION TO EXPERIMENTAL PROGRAMS

On the whole, a reduction in uncertainty will enhance our ability to detect smaller effects. In this study

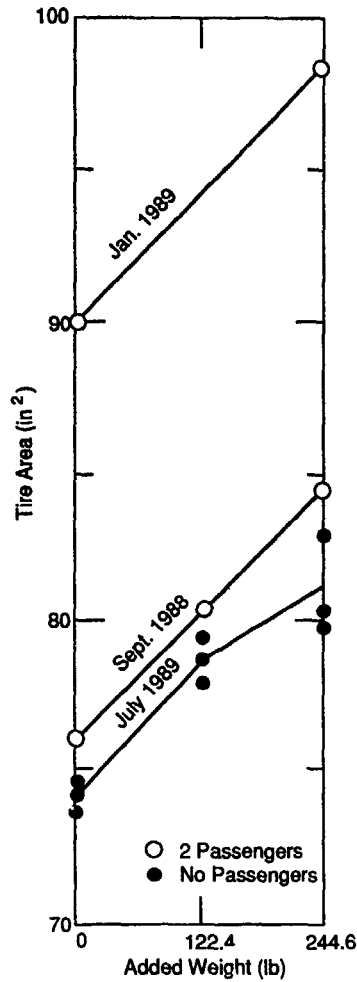


Figure 16. Tire contact areas at various vehicle load conditions (15-psi inflation pressure).

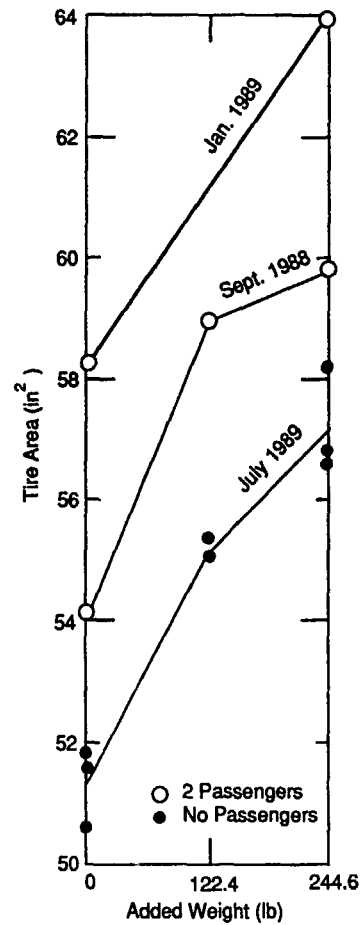


Figure 17. Tire contact areas at various vehicle load conditions (26-psi inflation pressure).

Table 10. Deflection from weight on bumper at two tire pressures.

Undeformed section width = 9 in., undeformed section height = 6.44 in., undeformed tire diameter = 29 in., tire tread void ratio = 0.44. Data taken September 1988.

| Tire pressure (psi) | Weights added on bumper (lbf) | Vertical load on wheel (lbf) | Deflected section height (in.) | Deflected section width (in.) | Deflection | | Contact area (in. ²) |
|---------------------|-------------------------------|------------------------------|--------------------------------|-------------------------------|------------|------|----------------------------------|
| | | | | | (in.) | (%) | |
| 26 | 0 | 1479 | 4.63 | 10.13 | 1.82 | 28.3 | 54.1 |
| | 122.4 | 1581 | 4.56 | 10.19 | 1.88 | 29.2 | 58.9 |
| | 244.6 | 1663 | 4.50 | 10.25 | 1.94 | 30.1 | 59.8 |
| 15 | 0 | 1422 | 4.00 | 10.75 | 2.44 | 37.9 | 76.0 |
| | 122.4 | 1533 | 3.88 | 10.19 | 2.56 | 39.8 | 80.3 |
| | 244.6 | 1634 | 3.75 | 11.00 | 2.69 | 41.8 | 84.4 |

I have identified sources of systematic error, quantified their effects and made suggestions to help reduce them (for example, using the recommended calibration method and data collection procedures). Based on a compilation of hard surface motion resistance measurements taken over the last several years, shown in Table 4, the change from a static to a rolling vehicle calibration procedure can reduce the standard deviation of the hard surface motion resistance by an average of 30%. This relates to being able to detect a variable that causes a smaller effect on motion resistance. Even greater improvement can be made by carefully controlling temperature, speed and weight distribution to eliminate their effects as discussed earlier.

Using the standard deviations from hard surface rolling resistance calculated in Table 4, we can determine the size of the detectable effect δ and calculate the decrease in δ caused by a decrease in the standard deviation. Rewriting eq 2

$$\delta = \sqrt{t^2 S_y^2 / n}$$

From statistics tables, the t value for a two-tailed test with two degrees of freedom and 95% confidence is

4.303. Based on a static calibration method, the standard deviation of the hard surface rolling resistance at 26 psi inflation pressure is $S_y = 4.6$ lbf (pooled standard deviation for left and right wheel). For three repetitions ($n = 3$), the smallest detectable effect δ equals 11.4 lbf. For the same tire and inflation pressure, a rolling calibration reduces the standard deviation to $S_y = 2.9$ (left and right wheel pooled), which reduces the detectable effect to 7.2 lbf. Simply put, a 37% decrease in the standard deviation decreases the detectable effect by the same percentage.

On deformable terrain (such as snow and soil), the standard deviation of the resistance measurements ranges primarily from approximately 15 to 60 lbf. For the standard three replicates, the smallest detectable effects range from 37 to 149 lbf. Therefore, detecting smaller effects on deformable terrain requires more repetitions or changing the experimental technique to reduce uncertainty.

To aid in experimental decision making, this type of information can be expressed either in tables or as operating characteristic (OC) curves. Figure 18 shows a set of operating characteristic curves for determining the probability of detecting an effect of size δ with 95%

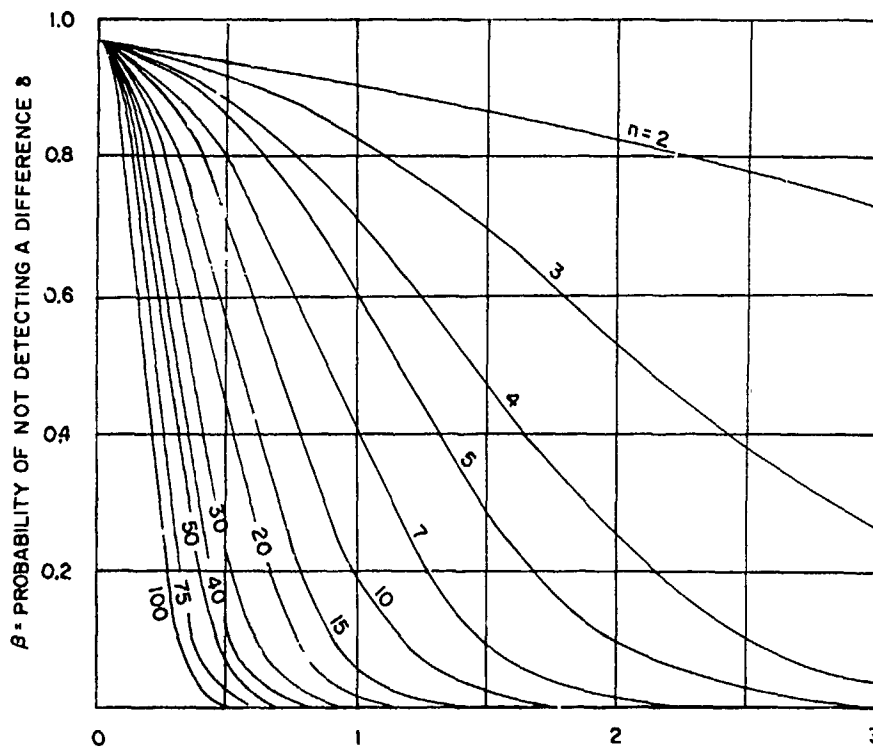


Figure 18. Operating Characteristic curves for a two-tailed t-test with 95% confidence (Natrella 1963). σ_y , the true standard deviation, can be approximated by S_y , the sample standard deviation.

confidence (from Natrella 1963). Using Figure 18, for a given number of replicates, n , we can determine the probability of not detecting a difference δ when a difference does in fact exist. This probability of not detecting a difference when one exists is called an Error of the Second Kind, β . These types of curves can be used for choosing the value of n for the results desired, for evaluating the effects of the size of the standard deviation, or for determining the consequences of underestimating the size of the true standard deviation.

SUMMARY AND CONCLUSIONS

In summary, it is important to know the precision of an experimental procedure so that an experiment can be planned to optimize the experimental results and minimize the time and cost of obtaining the data. The experimental error, or precision, can be expressed as the standard deviation, and can be estimated from previous data if it is not known. In this study, standard deviations were calculated from traction and motion resistance tests for a wide range of conditions (hard surface, snow and freezing and thawing soil).

Experimental error consists of both random error and systematic error. Precision can be improved by eliminating the systematic errors and reducing random errors. This study concentrated on improving technique by defining or eliminating systematic errors.

The systematic errors identified in this study were calibration method, temperature, vehicle speed, and weight distribution as reflected in the tire contact area. The results are outlined below.

1. Of the vehicle calibration techniques used, the rolling calibration is the most consistent; therefore, this is the preferred technique. Since the hard surface rolling resistance is used as the zero datum in this technique, the measured resistance reflects that caused by terrain deformation. A static calibration must be used to measure the total resistance.

2. Temperature changes affect the load cell readings, and temperature fluctuations inside the vehicle can affect the signal conditioning equipment, causing drift in the readings. The vehicle and all equipment should be operating and temperatures stabilized before vehicle calibration and testing begins.

3. Rolling resistance is a function of speed even at the low speeds commonly used in our test program. In the range of speeds tested, however, the average effect of speed is only about 0.3 lbf/mph.

4. The load on the front axles of the vehicle is extremely sensitive to the weight distribution in the vehicle. Small variations in the weight distribution are

also reflected in the contact area of the tires, which are kept at a constant inflation pressure rather than constant deflection. Although it is preferable to perform tests based on inflation pressure, care should be taken to maintain constant deflection.

This study has documented the precision of the CRREL Instrumented Vehicle and suggests techniques to eliminate some of the systematic errors associated with the data collection. Although the analysis was performed using data from the CRREL Instrumented Vehicle, the results are of use to anyone interested in performing precision mobility testing. As a result of this study a new vehicle calibration and test procedure is recommended. This procedure, along with guidelines for maintaining measurement accuracy throughout mobility testing, is detailed below.

1. Before testing, allow the vehicle to "soak" with the engine and electronics on, in the test environment until temperatures both inside and outside the vehicle stabilize. It is necessary for the vehicle temperatures to equilibrate with the ambient air and the heat of the engine. It also allows the temperature inside the vehicle to equilibrate and therefore, the electronics to stabilize. If the weather changes significantly during the course of the tests it should be noted and the vehicle should be recalibrated. Temperature can be monitored using thermocouples at various places inside and outside the vehicle. Temperature readings should be periodically recorded.

2. Choose the method of calibration (air, static or rolling) that best suits the experimental needs. Although the rolling calibration method is the most consistent, the other methods may be desirable for other test purposes. Calibrate the vehicle on as level and smooth a surface as possible. Since the load cells are very sensitive to the load distribution (and, therefore, tilt) of the vehicle, even very small slopes affect load transfer on the wheels.

3. Mobility testing procedures should routinely include a hard surface motion resistance measurement for each set of test conditions. This should be performed immediately prior to or after mobility testing on deformable terrain, and for each tire inflation pressure used. The hard surface information will serve as a base line for the mobility measurements taken throughout the day. Any changes in the hard surface values will indicate systematic errors that can then be corrected using the hard surface values as a reference base. In addition, the hard surface values can be subtracted from the gross resistance values to obtain that part of resistance caused by terrain deformation only.

4. Record the time of the calibration and of the subsequent tests. Additional information that should be

| | |
|---|------------------|
| Names of personnel: _____ | |
| _____ | |
| Date _____ | Location _____ |
| Weather _____ | |
| Conditions _____ | |
| Terrain Information: | |
| <input type="checkbox"/> snow/thaw depth _____ | |
| <input type="checkbox"/> 3-6 samples for moisture and density | |
| <input type="checkbox"/> sample for grain size | |
| <input type="checkbox"/> cone index | |
| <input type="checkbox"/> strength test (or samples) | |
| Calibration type, speed, time: _____ | |
| Base vehicle _____ | Tire _____ |
| speed _____ | Type _____ |
| Tire _____ | Tire _____ |
| inflation _____ | deflection _____ |
| A full test sequence will include: | |
| 1 hard surface rolling resistance, | |
| 3 traction tests, and | |
| 3 resistance tests. | |
| Any missing information will yield unusable test results. | |

Figure 19. Mobility testing checklist.

recorded for each test series includes calibration method (if rolling, at what speed) temperatures measured on or in vehicle, speed of tests, etc. A data checklist is given in Figure 19 and can be used to ensure that the necessary information is recorded.

LITERATURE CITED

- Berliner, E. and S. Shoop (1991) Instrumentation for vehicle mobility testing in the Frost Effects Research Facility. *Proceedings of the Second International Symposium on the State of the Art of Pavement Response Monitoring Systems for Roads and Airfields, Lebanon, N.H.*, American Society of Civil Engineers.
- Blaisdell, G.L. (1983) The CRREL Instrumented Vehicle: Hardware and software. USA Cold Regions Research and Engineering Laboratory, Special Report 83-3.
- Blaisdell, G.L., E.J. Chamberlain, and M. Mellor (1987) Evaluation of the cold regions aspects of mobility and hardening of the mobile test bed at Malmstrom Air Force Base. Final Report for the U.S. Air Force, Ballistic Missile Office, USA Cold Regions Research and Engineering Laboratory (unpublished).
- Clark, S. K. (1982) Mechanics of pneumatic tires. U.S. Department of Transportation, National Highway Traffic Safety Administration, U.S. Government Printing Office, 363-904 00-82-2, 931 p.
- Natrella, M.G. (1963) Experimental statistics. National Bureau of Standards Handbook 91, U.S. Government Printing Office.
- Pearson, E. S. and H.O. Hartley, Eds. (1966) *Biometrika Tables of Statisticians*. Cambridge: Cambridge University Press.
- Richmond, P.W., G.L. Blaisdell and C.E. Green (1990) Wheels and tracks in snow: Second validation study of the CRREL shallow snow mobility model. USA Cold Regions Research and Engineering Laboratory, CRREL Report no.90-13.
- Shoop, S.A. (1989) Vehicle mobility on thawing soils: Interim report on CRREL's test program. Cold Regions Research and Engineering Laboratory, Special Report 89-31.
- Shoop, S.A. (1990) Mechanisms controlling vehicle mobility on a thawing soil. *Proceedings of the 10th International Conference of the International Society of Terrain-Vehicle Systems, Kobe, Japan, Aug. 1990*. Vol. I, p 301-312.
- Youden, W.J. and E.H. Steiner (1984) Statistical manual of the Association of Official Analytical Chemists. Arlington, Virginia: Association of Official Analytical Chemists.

APPENDIX A: Range Test for Homogeneity of Variance.

A range test is used to check the "homogeneity" or likeness of data sets. The variances of the groups of data are considered homogenous if the ratio of the maximum range to the sum of the ranges does not exceed the value obtained from the table below. For 15 data sets ($k = 15$) with at least 4 replicates in each set ($n = 4$) the ratio obtained from the table is 0.15. Since this is greater than the calculated ratio, the data sets are homogenous (and their standard deviations can be pooled).

If the left and right side values are combined, the calculated ratio is 0.064 and the table value is 0.08. Again, the data are homogeneous.

Table A1. Ranges from traction data sets collected in Montana, March 1987.

| Date 1987 | Conditions | Range | | No. of tests |
|--------------|-------------------------------|-------|-------|--------------|
| | | Left | Right | |
| 3/12 | dry soil, 15 psi | 0.082 | 0.126 | 9 |
| 3/12 | dry soil, 15 psi | 0.021 | 0.058 | 4 |
| 3/13 | lt. rain on soil, 15 psi | 0.036 | 0.049 | 5 |
| 3/13 | 1/16 in. rain on soil, 15 psi | 0.064 | 0.062 | 5 |
| 3/17 | dry soil, 15 psi | 0.063 | 0.107 | 6 |
| 3/17 | dry soil, 26 psi | 0.078 | 0.066 | 6 |
| 3/17 | dry soil, 26 psi | 0.050 | 0.167 | 6 |
| 3/19 | 7 in. snow, 26 psi | 0.110 | 0.088 | 6 |
| 3/19 | 7 in. snow, 15 psi | 0.059 | 0.064 | 5 |
| 3/19 | 10 in. snow, 15 psi | 0.062 | 0.044 | 6 |
| 3/19 | 11 in. snow, 15 psi | 0.092 | 0.046 | 6 |
| 3/21 | 6 in. snow, 15 psi | 0.034 | 0.086 | 5 |
| 3/21 | 6 in. snow, 26 psi | 0.064 | 0.036 | 8 |
| 3/21 | slushy, 26 psi | 0.034 | 0.048 | 4 |
| 3/21 | slushy, 15 psi | 0.039 | 0.081 | 4 |
| | SUM | 0.888 | 1.027 | 85 |
| | MAX. RANGE | 0.110 | 0.126 | |
| | RATIO MAX/SUM | 0.124 | 0.123 | |

Table A2. Criterion for testing homogeneity of variation from ranges with 95% confidence (from Youden and Steiner 1984).

| No. of values in each range (n) | No. of ranges compared (k) | | | | | | | | | | | | | | |
|---|----------------------------|------|------|------|------|------|------|------|------|------|------|------|------|------|------|
| | 2 | 3 | 4 | 5 | 6 | 7 | 8 | 9 | 10 | 12 | 15 | 20 | 30 | 40 | 50 |
| 2 | 0.96 | 0.81 | 0.68 | 0.58 | 0.51 | 0.45 | 0.41 | 0.37 | 0.34 | 0.29 | 0.24 | 0.19 | 0.13 | 0.10 | 0.08 |
| 3 | 0.86 | 0.67 | 0.54 | 0.45 | 0.39 | 0.34 | 0.31 | 0.28 | 0.25 | 0.22 | 0.18 | 0.14 | 0.10 | 0.07 | 0.06 |
| 4 | 0.80 | 0.60 | 0.48 | 0.40 | 0.34 | 0.30 | 0.27 | 0.24 | 0.22 | 0.19 | 0.15 | 0.12 | 0.08 | 0.06 | 0.05 |
| 5 | 0.76 | 0.56 | 0.45 | 0.37 | 0.32 | 0.28 | 0.25 | 0.22 | 0.20 | 0.17 | 0.14 | 0.11 | 0.08 | 0.06 | 0.05 |
| 6 | 0.74 | 0.54 | 0.42 | 0.35 | 0.30 | 0.26 | 0.23 | 0.21 | 0.19 | 0.16 | 0.13 | 0.10 | 0.07 | 0.05 | 0.04 |
| 7 | 0.72 | 0.52 | 0.41 | 0.34 | 0.29 | 0.25 | 0.22 | 0.20 | 0.18 | 0.16 | 0.13 | 0.10 | 0.07 | 0.05 | 0.04 |
| 8 | 0.70 | 0.51 | 0.40 | 0.33 | 0.28 | 0.24 | 0.22 | 0.20 | 0.18 | 0.15 | 0.12 | 0.10 | 0.07 | 0.05 | 0.04 |
| 9 | 0.69 | 0.50 | 0.39 | 0.32 | 0.27 | 0.24 | 0.21 | 0.19 | 0.17 | 0.15 | 0.12 | 0.09 | 0.06 | 0.05 | 0.04 |
| 10 | 0.68 | 0.49 | 0.38 | 0.31 | 0.27 | 0.23 | 0.21 | 0.19 | 0.17 | 0.15 | 0.12 | 0.09 | 0.06 | 0.05 | 0.04 |

Table A3. Peak traction values for various terrain conditions tested in Montana, March 1987.

| <i>CONDITIONS</i> | <i>TEST #</i> | <i>PEAK TRACTION</i> | |
|-----------------------------|---------------|----------------------|--------------|
| | | <i>LEFT</i> | <i>RIGHT</i> |
| dry, 15psi tire D | 0312C | 0.505 | 0.473 |
| | 0312D | 0.540 | 0.532 |
| | 0312E | 0.553 | 0.562 |
| | 0312F | 0.587 | 0.549 |
| | 0312G | 0.530 | 0.551 |
| | 0312H | 0.521 | 0.526 |
| | 0312I | 0.535 | 0.599 |
| | 0312J | 0.550 | 0.573 |
| | 0312K | 0.559 | 0.566 |
| ----- | | | |
| MEAN | | 0.542 | 0.548 |
| STANDARD DEVIATION | | 0.024 | 0.036 |
| ----- | | | |
| dry, 15psi tire D | 0312L | 0.566 | 0.633 |
| | 0312M | 0.576 | 0.587 |
| | 0312N | 0.586 | 0.645 |
| | 0312O | 0.565 | 0.631 |
| ----- | | | |
| MEAN | | 0.573 | 0.624 |
| STANDARD DEVIATION | | 0.010 | 0.025 |
| ----- | | | |
| lt. rain 15 psi tire D | 0313C | 0.548 | 0.516 |
| | 0313D | 0.534 | 0.511 |
| | 0313E | 0.519 | 0.492 |
| | 0313F | 0.512 | 0.541 |
| | 0313G | 0.537 | 0.539 |
| ----- | | | |
| MEAN | | 0.530 | 0.520 |
| STANDARD DEVIATION | | 0.014 | 0.021 |
| ----- | | | |
| 1/16" rain 15 psi tire D | 0313H | 0.601 | 0.587 |
| | 0313I | 0.603 | 0.573 |
| | 0313J | 0.587 | 0.591 |
| | 0313K | 0.596 | 0.590 |
| | 0313L | 0.651 | 0.635 |
| ----- | | | |
| MEAN | | 0.608 | 0.595 |
| STANDARD DEVIATION | | 0.025 | 0.023 |
| ----- | | | |

Table A3 (Cont'd).

| CONDITIONS | TEST # | PEAK TRACTION | |
|-----------------------------|----------|---------------|-------|
| | | LEFT | RIGHT |
| dry, 15 psi tire D | 0317A | 0.717 | 0.699 |
| | 0317B | 0.706 | 0.681 |
| | 0317C | 0.769 | 0.788 |
| | 0317D | 0.738 | 0.751 |
| | 0317E | 0.721 | 0.706 |
| | 0317G | 0.718 | 0.703 |
| | MEAN | | 0.728 |
| STANDARD DEVIATION | | 0.023 | 0.040 |
| dry, 26 psi tire D | 0317M | 0.669 | 0.684 |
| | 0317N | 0.666 | 0.698 |
| | 0317O | 0.674 | 0.665 |
| | 0317P | 0.699 | 0.697 |
| | 0317Q | 0.724 | 0.730 |
| | 0317R | 0.752 | 0.731 |
| | MEAN | | 0.697 |
| STANDARD DEVIATION | | 0.035 | 0.026 |
| dry, 26 psi tire D | 0317S | 0.715 | 0.749 |
| | 0317T | 0.755 | 0.737 |
| | 0317U | 0.705 | 0.682 |
| | 0317V | 0.739 | 0.729 |
| | 0317W | 0.725 | 0.714 |
| | 0317X | 0.741 | 0.748 |
| MEAN | | 0.730 | 0.727 |
| STANDARD DEVIATION | | 0.018 | 0.025 |
| 7 in. snow, 26psi tire D | 0319K | 0.339 | 0.326 |
| | 0319L | 0.302 | 0.317 |
| | 0319M | 0.306 | 0.311 |
| | 0319O | 0.229 | 0.238 |
| | 0319P | 0.267 | 0.244 |
| | 0319Q | 0.289 | 0.251 |
| MEAN | | 0.289 | 0.281 |
| STANDARD DEVIATION | 0.034257 | 0.038 | 0.041 |

Table A3 (Cont'd). Peak traction values for various terrain conditions tested in Montana, March 1987.

| <i>CONDITIONS</i> | <i>TEST #</i> | <i>PEAK TRACTION</i> | |
|-------------------------------|---------------|----------------------|--------------|
| | | <i>LEFT</i> | <i>RIGHT</i> |
| 7 in. snow, 15psi tire D | 0319T | 0.275 | 0.295 |
| | 0319U | 0.334 | 0.356 |
| | 0319V | 0.301 | 0.274 |
| | 0319W | 0.279 | 0.316 |
| | 0319X | 0.296 | 0.292 |
| ----- | | | |
| MEAN | | 0.279 | 0.307 |
| STANDARD DEVIATION | | 0.023 | 0.031 |
| ----- | | | |
| 10 in. snow, 15 psi tire D | 0319c | 0.291 | 0.293 |
| | 0319d | 0.319 | 0.269 |
| | 0319e | 0.293 | 0.258 |
| | 0319f | 0.323 | 0.287 |
| | 0319g | 0.336 | 0.276 |
| | 0319h | 0.353 | 0.249 |
| ----- | | | |
| MEAN | | 0.319 | 0.272 |
| STANDARD DEVIATION | | 0.024 | 0.017 |
| ----- | | | |
| 11 in. snow, 15 psi tire D | 0319k | 0.333 | 0.235 |
| | 0319l | 0.277 | 0.189 |
| | 0319m | 0.311 | 0.222 |
| | 0319n | 0.328 | 0.228 |
| | 0319o | 0.306 | 0.222 |
| | 0319p | 0.369 | 0.218 |
| ----- | | | |
| MEAN | | 0.321 | 0.219 |
| STANDARD DEVIATION | | 0.031 | 0.016 |
| ----- | | | |
| 6 in. snow, 15 psi tire D | 0321R | 0.404 | 0.486 |
| | 0321S | 0.422 | 0.461 |
| | 0321T | 0.413 | 0.412 |
| | 0321U | 0.428 | 0.436 |
| | 0321V | 0.394 | 0.400 |
| ----- | | | |
| MEAN | | 0.412 | 0.439 |
| STANDARD DEVIATION | | 0.014 | 0.035 |
| ----- | | | |

Table A3 (Cont'd).

| <i>CONDITIONS</i> | <i>TEST #</i> | <i>PEAK TRACTION</i> | |
|--|---------------|----------------------|--------------|
| | | <i>LEFT</i> | <i>RIGHT</i> |
| 6 in. snow, 26 psi tire D | 0321A | 0.435 | 0.338 |
| | 0321B | 0.394 | 0.335 |
| | 0321C | 0.371 | 0.342 |
| | 0321D | 0.413 | 0.359 |
| | 0321E | 0.374 | 0.346 |
| | 0321F | 0.400 | 0.371 |
| | 0321G | 0.378 | 0.356 |
| | 0321H | 0.379 | 0.356 |
| ----- | | | |
| MEAN | | 0.393 | 0.350 |
| STANDARD DEVIATION | | 0.022 | 0.012 |
| ----- | | | |
| slushy snow on gravel road, 26 psi tire D | 0321I | 0.680 | 0.666 |
| | 0321P | 0.714 | 0.682 |
| | 0321Q | 0.702 | 0.714 |
| | 0321R | 0.689 | 0.694 |
| ----- | | | |
| MEAN | | 0.696 | 0.689 |
| STANDARD DEVIATION | | 0.015 | 0.020 |
| ----- | | | |
| slushy snow on gravel road, 15 psi, tire D | 0321S | 0.661 | 0.646 |
| | 0321T | 0.679 | 0.655 |
| | 0321U | 0.640 | 0.624 |
| | 0321V | 0.677 | 0.705 |
| ----- | | | |
| MEAN | | 0.664 | 0.658 |
| STANDARD DEVIATION | | 0.018 | 0.034 |
| ----- | | | |

Appendix B: Calibration files for experiments evaluating the repeatability of calibration methods.

TABLE OF CONTENTS

| <i>Calibration Test #</i> | <i>Calibration Type</i> | <i>Calibration Test #</i> | <i>Calibration Type</i> |
|---------------------------|-------------------------|---------------------------|-------------------------|
| C1018A | AIR | C1019A | AIR |
| C1018B | STATIC | C1019B | STATIC |
| C1018C | ROLLING | C1019C | AIR |
| C1018D | AIR | C1019D | STATIC |
| C1018E | ROLLING | C1019E | STATIC |
| C1018F | ROLLING | C1019F | STATIC |
| C1018G | ROLLING | C1019G | ROLLING |
| C1018H | AIR | C1019H | ROLLING |
| C1018I | AIR | C1019I | AIR |
| C1018J | STATIC | C1019J | STATIC |
| C1018K | ROLLING | C1019K | ROLLING |
| C1018L | ROLLING | C1019L | STATIC |
| C1018M | STATIC | C1019M | AIR |
| C1018N | AIR | C1019O | AIR |
| C1018O | ROLLING | C1019P | ROLLING |
| C1018P | STATIC | C1019Q | ROLLING |
| C1018Q | STATIC | C1019R | ROLLING |
| C1018R | STATIC | C1019S | AIR |
| C1018S | AIR | C1019T | ROLLING |
| C1018T | STATIC | C1019U | STATIC |
| C1018U | AIR | C1019V | AIR |

CALIBRATION FILE: C1018A

| | <i>Zero Value</i> | <i>Shunt Value</i> | <i>Scale Value</i> |
|----------------------|-------------------|--------------------|--------------------|
| Left Vertical | -941.21 | 258.71 | 0.8726 |
| Left Longitudinal | -51.50 | 1151.25 | 0.8581 |
| Left Side | -437.33 | 1949.71 | 0.8948 |
| Left Velocity | 9.13 | 269.79 | 0.0192 |
| Right Vertical | -686.67 | 517.92 | 0.8816 |
| Right Longitudinal | -27.33 | 1175.58 | 0.8743 |
| Right Side | -377.42 | 2018.88 | 1.0011 |
| Right Velocity | 17.00 | 279.54 | 0.0190 |
| Sonic Devc. Velocity | 9.67 | 9.67 | NA |
| Fifth-Wheel Velocity | 8.25 | 269.63 | 0.0191 |

CALIBRATION FILE: C1018B

| | <i>Zero Value</i> | <i>Shunt Value</i> | <i>Scale Value</i> |
|----------------------|-------------------|--------------------|--------------------|
| Left Vertical | -939.92 | 259.42 | 0.8730 |
| Left Longitudinal | -41.75 | 1161.54 | 0.8581 |
| Left Side | -402.54 | 1983.75 | 0.8951 |
| Left Velocity | 9.83 | 282.88 | 0.0183 |
| Right Vertical | -690.58 | 513.75 | 0.8818 |
| Right Longitudinal | 27.79 | 1230.63 | 0.8742 |
| Right Side | -355.63 | 2046.79 | 0.9986 |
| Right Velocity | 17.92 | 292.29 | 0.0182 |
| Sonic Devc. Velocity | 10.13 | 10.00 | NA |
| Fifth-Wheel Velocity | 9.125 | 283.17 | 0.0182 |

CALIBRATION FILE: C1018C

| | <i>Zero Value</i> | <i>Shunt Value</i> | <i>Scale Value</i> |
|----------------------|-------------------|--------------------|--------------------|
| Left Vertical | -945.38 | 254.67 | 0.8725 |
| Left Longitudinal | -55.83 | 1152.29 | 0.8577 |
| Left Side | -406.71 | 1987.88 | 0.8954 |
| Left Velocity | 64.46 | 270.25 | 0.0243 |
| Right Vertical | -700.75 | 509.17 | 0.8777 |
| Right Longitudinal | 24.83 | 1225.33 | 0.8736 |
| Right Side | -351.29 | 2047.00 | 1.0003 |
| Right Velocity | 70.88 | 279.33 | 0.0240 |
| Sonic Devc. Velocity | 10.96 | 10.67 | NA |
| Fifth-Wheel Velocity | 62.58 | 270.50 | 0.0240 |

CALIBRATION FILE: C1018D

| | <i>Zero Value</i> | <i>Shunt Value</i> | <i>Scale Value</i> |
|----------------------|-------------------|--------------------|--------------------|
| Left Vertical | -944.54 | 255.92 | 0.8722 |
| Left Longitudinal | -49.58 | 1153.13 | 0.8574 |
| Left Side | -445.13 | 1945.01 | 0.8936 |
| Left Velocity | 10.00 | 259.46 | 0.0200 |
| Right Vertical | -701.75 | 498.25 | 0.885 |
| Right Longitudinal | -26.17 | 1176.92 | 0.8737 |
| Right Side | -380.04 | 2047.00 | 0.9884 |
| Right Velocity | 17.50 | 268.79 | 0.0199 |
| Sonic Devc. Velocity | 10.25 | 10.46 | NA |
| Fifth-Wheel Velocity | 8.75 | 260.58 | 0.0199 |

CALIBRATION FILE: C1018E

| | <i>Zero Value</i> | <i>Shunt Value</i> | <i>Scale Value</i> |
|----------------------|-------------------|--------------------|--------------------|
| Left Vertical | -942.83 | 257.50 | 0.8723 |
| Left Longitudinal | -59.58 | 1143.33 | 0.8578 |
| Left Side | -401.13 | 1991.86 | 0.8926 |
| Left Velocity | 64.13 | 271.50 | 0.0241 |
| Right Vertical | -698.83 | 506.42 | 0.8811 |
| Right Longitudinal | 21.96 | 1222.58 | 0.8739 |
| Right Side | -343.79 | 2047.00 | 1.0034 |
| Right Velocity | 72.63 | 280.50 | 0.0249 |
| Sonic Devc. Velocity | 10.79 | 11.00 | NA |
| Fifth-Wheel Velocity | 63.71 | 272.13 | 0.0240 |

CALIBRATION FILE: C1018F

| | <i>Zero Value</i> | <i>Shunt Value</i> | <i>Scale Value</i> |
|----------------------|-------------------|--------------------|--------------------|
| Left Vertical | -943.46 | 257.25 | 0.8720 |
| Left Longitudinal | -60.92 | 1142.50 | 0.8577 |
| Left Side | -404.79 | 1988.83 | 0.8924 |
| Left Velocity | 67.04 | 265.86 | 0.0251 |
| Right Vertical | -702.79 | 529.21 | 0.8620 |
| Right Longitudinal | 18.71 | 1221.54 | 0.8737 |
| Right Side | -344.92 | 2047.00 | 1.0030 |
| Right Velocity | 74.13 | 274.83 | 0.0249 |
| Sonic Devc. Velocity | 10.88 | 11.04 | NA |
| Fifth-Wheel Velocity | 65.63 | 266.46 | 0.0249 |

CALIBRATION FILE: C1018G

| | <i>Zero Value</i> | <i>Shunt Value</i> | <i>Scale Value</i> |
|----------------------|-------------------|--------------------|--------------------|
| Left Vertical | -942.88 | 257.33 | 0.8723 |
| Left Longitudinal | -61.46 | 1144.79 | 0.8578 |
| Left Side | -402.50 | 1983.92 | 0.8951 |
| Left Velocity | 63.33 | 260.08 | 0.0254 |
| Right Vertical | -702.17 | 499.29 | 0.8839 |
| Right Longitudinal | 20.54 | 1226.04 | 0.8740 |
| Right Side | -351.88 | 2047.00 | 1.0001 |
| Right Velocity | 73.08 | 268.83 | 0.0255 |
| Sonic Devc. Velocity | 11.21 | 11.42 | NA |
| Fifth-Wheel Velocity | 64.17 | 261.54 | 0.0253 |

CALIBRATION FILE: C1018H

| | <i>Zero Value</i> | <i>Shunt Value</i> | <i>Scale Value</i> |
|----------------------|-------------------|--------------------|--------------------|
| Left Vertical | -943.67 | 257.21 | 0.8719 |
| Left Longitudinal | -51.38 | 1151.00 | 0.8576 |
| Left Side | -447.63 | 1942.92 | 0.8935 |
| Left Velocity | 10.21 | 254.58 | 0.0205 |
| Right Vertical | -703.58 | 499.33 | 0.8829 |
| Right Longitudinal | -30.13 | 1172.29 | 0.8741 |
| Right Side | -380.92 | 2047.00 | 0.9881 |
| Right Velocity | 17.83 | 264.29 | 0.0203 |
| Sonic Devc. Velocity | 10.83 | 11.54 | NA |
| Fifth-Wheel Velocity | 9.92 | 255.83 | 0.0203 |

CALIBRATION FILE: C1018I

| | <i>Zero Value</i> | <i>Shunt Value</i> | <i>Scale Value</i> |
|----------------------|-------------------|--------------------|--------------------|
| Left Vertical | -944.33 | 255.58 | 0.8725 |
| Left Longitudinal | -52.63 | 1149.92 | 0.8579 |
| Left Side | -448.88 | 1941.50 | 0.8936 |
| Left Velocity | 10.13 | 277.08 | 0.0187 |
| Right Vertical | -702.67 | 500.46 | 0.8827 |
| Right Longitudinal | -29.13 | 1173.54 | 0.8743 |
| Right Side | -379.92 | 2004.17 | 1.0062 |
| Right Velocity | 17.92 | 286.17 | 0.0186 |
| Sonic Devc. Velocity | 10.83 | 11.25 | NA |
| Fifth-Wheel Velocity | 9.96 | 278.50 | 0.0186 |

CALIBRATION FILE: C1018J

| | <i>Zero Value</i> | <i>Shunt Value</i> | <i>Scale Value</i> |
|----------------------|-------------------|--------------------|--------------------|
| Left Vertical | -944.17 | 256.42 | 0.8721 |
| Left Longitudinal | -45.21 | 1157.96 | 0.8577 |
| Left Side | -413.88 | 1974.79 | 0.8942 |
| Left Velocity | 10.04 | 264.54 | 0.0196 |
| Right Vertical | -702.25 | 501.21 | 0.8825 |
| Right Longitudinal | 27.58 | 1230.79 | 0.8741 |
| Right Side | -369.25 | 2011.83 | 1.0075 |
| Right Velocity | 18.21 | 273.54 | 0.0196 |
| Sonic Devc. Velocity | 10.21 | 10.92 | NA |
| Fifth-Wheel Velocity | 10.38 | 265.38 | 0.0196 |

CALIBRATION FILE: C1018K

| | <i>Zero Value</i> | <i>Shunt Value</i> | <i>Scale Value</i> |
|----------------------|-------------------|--------------------|--------------------|
| Left Vertical | -943.63 | 256.88 | 0.8721 |
| Left Longitudinal | -60.13 | 1143.04 | 0.8577 |
| Left Side | -409.63 | 1986.75 | 0.8913 |
| Left Velocity | 64.92 | 264.63 | 0.0250 |
| Right Vertical | -703.63 | 500.50 | 0.8820 |
| Right Longitudinal | 18.54 | 1222.21 | 0.8739 |
| Right Side | -336.83 | 2044.29 | 1.0075 |
| Right Velocity | 73.71 | 273.42 | 0.0250 |
| Sonic Devc. Velocity | 10.96 | 11.29 | NA |
| Fifth-Wheel Velocity | 65.58 | 266.54 | 0.0249 |

CALIBRATION FILE: C1018L

| | <i>Zero Value</i> | <i>Shunt Value</i> | <i>Scale Value</i> |
|----------------------|-------------------|--------------------|--------------------|
| Left Vertical | -942.46 | 257.71 | 0.8724 |
| Left Longitudinal | -58.79 | 1144.46 | 0.8579 |
| Left Side | -407.92 | 1985.75 | 0.8924 |
| Left Velocity | 63.25 | 256.21 | 0.0259 |
| Right Vertical | -702.29 | 501.29 | 0.8824 |
| Right Longitudinal | 19.75 | 1219.29 | 0.8740 |
| Right Side | -343.79 | 2035.58 | 1.0082 |
| Right Velocity | 72.96 | 266.00 | 0.0259 |
| Sonic Devc. Velocity | 11.33 | 11.29 | NA |
| Fifth-Wheel Velocity | 64.17 | 257.63 | 0.0258 |

CALIBRATION FILE: C1018M

| | <i>Zero Value</i> | <i>Shunt Value</i> | <i>Scale Value</i> |
|----------------------|-------------------|--------------------|--------------------|
| Left Vertical | -942.79 | 257.42 | 0.8723 |
| Left Longitudinal | -45.00 | 1158.38 | 0.8578 |
| Left Side | -428.88 | 1960.21 | 0.8941 |
| Left Velocity | 10.29 | 255.79 | 0.0204 |
| Right Vertical | -702.75 | 498.08 | 0.8844 |
| Right Longitudinal | 45.92 | 1248.50 | 0.8740 |
| Right Side | -380.33 | 2000.00 | 1.0078 |
| Right Velocity | 18.29 | 265.75 | 0.0202 |
| Sonic Devc. Velocity | 11.29 | 11.13 | NA |
| Fifth-Wheel Velocity | 9.88 | 257.50 | 0.0202 |

CALIBRATION FILE: C1018N

| | <i>Zero Value</i> | <i>Shunt Value</i> | <i>Scale Value</i> |
|----------------------|-------------------|--------------------|--------------------|
| Left Vertical | -943.38 | 257.58 | 0.8716 |
| Left Longitudinal | -35.00 | 1149.92 | 0.8576 |
| Left Side | -453.54 | 1939.50 | 0.8926 |
| Left Velocity | 9.54 | 261.08 | 0.0199 |
| Right Vertical | -709.29 | 493.67 | 0.8828 |
| Right Longitudinal | -30.04 | 1172.42 | 0.8738 |
| Right Side | -381.42 | 2044.71 | 0.9888 |
| Right Velocity | 18.08 | 270.29 | 0.0198 |
| Sonic Devc. Velocity | 11.29 | 11.46 | NA |
| Fifth-Wheel Velocity | 10.33 | 263.63 | 0.0197 |

CALIBRATION FILE: C1018O

| | <i>Zero Value</i> | <i>Shunt Value</i> | <i>Scale Value</i> |
|----------------------|-------------------|--------------------|--------------------|
| Left Vertical | -943.63 | 256.25 | 0.8726 |
| Left Longitudinal | -58.04 | 1145.04 | 0.8580 |
| Left Side | -405.50 | 1987.50 | 0.8926 |
| Left Velocity | 63.79 | 249.17 | 0.0270 |
| Right Vertical | -710.67 | 490.71 | 0.8840 |
| Right Longitudinal | 19.92 | 1220.88 | 0.8738 |
| Right Side | -345.00 | 2039.75 | 1.0060 |
| Right Velocity | 71.42 | 257.42 | 0.0270 |
| Sonic Devc. Velocity | 11.17 | 11.21 | NA |
| Fifth-Wheel Velocity | 63.08 | 250.79 | 0.0270 |

CALIBRATION FILE: C1018P

| | <i>Zero Value</i> | <i>Shunt Value</i> | <i>Scale Value</i> |
|----------------------|-------------------|--------------------|--------------------|
| Left Vertical | -942.42 | 258.08 | 0.8721 |
| Left Longitudinal | -40.63 | 1162.42 | 0.8577 |
| Left Side | -459.67 | 1931.58 | 0.8933 |
| Left Velocity | 9.75 | 267.54 | 0.0194 |
| Right Vertical | -710.38 | 490.00 | 0.8847 |
| Right Longitudinal | 46.17 | 1248.21 | 0.8739 |
| Right Side | -409.04 | 1977.42 | 1.0053 |
| Right Velocity | 17.92 | 277.08 | 0.0193 |
| Sonic Devc. Velocity | 10.92 | 11.33 | NA |
| Fifth-Wheel Velocity | 9.96 | 269.08 | 0.0193 |

CALIBRATION FILE: C1018Q

| | <i>Zero Value</i> | <i>Shunt Value</i> | <i>Scale Value</i> |
|----------------------|-------------------|--------------------|--------------------|
| Left Vertical | -944.25 | 256.00 | 0.8723 |
| Left Longitudinal | -46.21 | 1157.13 | 0.8579 |
| Left Side | -426.58 | 1964.42 | 0.8934 |
| Left Velocity | 10.29 | 264.92 | 0.0196 |
| Right Vertical | -708.92 | 491.38 | 0.8848 |
| Right Longitudinal | 37.58 | 1239.96 | 0.8739 |
| Right Side | -385.13 | 2000.46 | 1.0056 |
| Right Velocity | 18.33 | 275.00 | 0.0195 |
| Sonic Devc. Velocity | 11.17 | 10.83 | NA |
| Fifth-Wheel Velocity | 10.08 | 265.79 | 0.0196 |

CALIBRATION FILE: C1018R

| | <i>Zero Value</i> | <i>Shunt Value</i> | <i>Scale Value</i> |
|----------------------|-------------------|--------------------|--------------------|
| Left Vertical | -943.54 | 256.75 | 0.8723 |
| Left Longitudinal | -43.96 | 1158.75 | 0.8579 |
| Left Side | -461.46 | 1929.38 | 0.8934 |
| Left Velocity | | 10.88 | 265.00 |
| 0.0197 | | | |
| Right Vertical | -708.50 | 492.67 | 0.8841 |
| Right Longitudinal | 45.54 | 1248.08 | 0.8737 |
| Right Side | -411.42 | 1973.46 | 1.0060 |
| Right Velocity | 18.38 | 273.08 | 0.0196 |
| Sonic Devc. Velocity | 11.21 | 11.38 | NA |
| Fifth-Wheel Velocity | 9.92 | 265.96 | 0.0195 |

CALIBRATION FILE: C1018S

| | <i>Zero Value</i> | <i>Shunt Value</i> | <i>Scale Value</i> |
|----------------------|-------------------|--------------------|--------------------|
| Left Vertical | -943.13 | 257.25 | 0.8722 |
| Left Longitudinal | -53.13 | 1149.50 | 0.8577 |
| Left Side | -452.92 | 1929.13 | 0.8930 |
| Left Velocity | 10.33 | 261.96 | 0.0199 |
| Right Vertical | -707.50 | 492.92 | 0.8847 |
| Right Longitudinal | -31.88 | 1170.50 | 0.8740 |
| Right Side | -380.88 | 2005.88 | 1.0051 |
| Right Velocity | 18.67 | 270.54 | 0.0200 |
| Sonic Devc. Velocity | 11.13 | 11.29 | NA |
| Fifth-Wheel Velocity | 9.83 | 262.33 | 0.0198 |

CALIBRATION FILE: C1018T

| | <i>Zero Value</i> | <i>Shunt Value</i> | <i>Scale Value</i> |
|----------------------|-------------------|--------------------|--------------------|
| Left Vertical | -944.25 | 255.29 | 0.8721 |
| Left Longitudinal | -33.96 | 1169.58 | 0.8577 |
| Left Side | -396.08 | 1994.42 | 0.8935 |
| Left Velocity | 10.58 | 268.54 | 0.0194 |
| Right Vertical | -706.83 | 492.96 | 0.8852 |
| Right Longitudinal | 35.50 | 1238.67 | 0.8738 |
| Right Side | -358.21 | 2028.08 | 1.0053 |
| Right Velocity | 18.75 | 276.88 | 0.0194 |
| Sonic Devc. Velocity | 11.38 | 11.54 | NA |
| Fifth-Wheel Velocity | 10.00 | 269.79 | 0.0192 |

CALIBRATION FILE: C1018U

| | <i>Zero Value</i> | <i>Shunt Value</i> | <i>Scale Value</i> |
|----------------------|-------------------|--------------------|--------------------|
| Left Vertical | -944.13 | 256.50 | 0.8720 |
| Left Longitudinal | -53.5 | 1149.33 | 0.8581 |
| Left Side | -454.29 | 1938.58 | 0.8927 |
| Left Velocity | 10.79 | 282.79 | 0.0184 |
| Right Vertical | -709.34 | 495.04 | 0.8847 |
| Right Longitudinal | -32.96 | 1169.58 | 0.8739 |
| Right Side | -379.54 | 2011.96 | 1.0031 |
| Right Velocity | 18.88 | 292.08 | 0.0183 |
| Sonic Devc. Velocity | 11.54 | 11.96 | NA |
| Fifth-Wheel Velocity | 10.5 | 284.08 | 0.0183 |

CALIBRATION FILE: C1019A

| | <i>Zero Value</i> | <i>Shunt Value</i> | <i>Scale Value</i> |
|----------------------|-------------------|--------------------|--------------------|
| Left Vertical | -949.83 | 250.13 | 0.8725 |
| Left Longitudinal | -64.42 | 1138.50 | 0.8578 |
| Left Side | -438.96 | 1941.59 | 0.8973 |
| Left Velocity | -6.21 | 244.50 | 0.0199 |
| Right Vertical | -687.33 | 514.00 | 0.8840 |
| Right Longitudinal | -40.29 | 1162.04 | 0.8744 |
| Right Side | -371.17 | 2047.00 | 0.9921 |
| Right Velocity | 1.63 | 255.29 | 0.0197 |
| Sonic Devc. Velocity | -5.08 | -5.13 | NA |
| Fifth-Wheel Velocity | -6.17 | 244.46 | 0.0200 |

CALIBRATION FILE: C1019B

| | <i>Zero Value</i> | <i>Shunt Value</i> | <i>Scale Value</i> |
|----------------------|-------------------|--------------------|--------------------|
| Left Vertical | -946.50 | 253.29 | 0.8727 |
| Left Longitudinal | -52.00 | 1151.75 | 0.8576 |
| Left Side | -393.46 | 1986.92 | 0.8973 |
| Left Velocity | -4.33 | 252.92 | 0.0194 |
| Right Vertical | -686.38 | 514.75 | 0.8842 |
| Right Longitudinal | 18.00 | 1220.63 | 0.8742 |
| Right Side | -368.71 | 2047.00 | 0.0199 |
| Right Velocity | 3.08 | 262.00 | 0.0193 |
| Sonic Devc. Velocity | -3.29 | -1.71 | NA |
| Fifth-Wheel Velocity | -4.83 | 253.75 | 0.0193 |

CALIBRATION FILE: C1019C

| | <i>Zero Value</i> | <i>Shunt Value</i> | <i>Scale Value</i> |
|----------------------|-------------------|--------------------|--------------------|
| Left Vertical | -944.50 | 255.42 | 0.8726 |
| Left Longitudinal | -55.67 | 1147.29 | 0.8575 |
| Left Side | -435.92 | 1947.75 | 0.8961 |
| Left Velocity | -0.83 | 255.04 | 0.0195 |
| Right Vertical | -686.67 | 514.00 | 0.8845 |
| Right Longitudinal | -33.58 | 1168.80 | 0.8740 |
| Right Side | -374.21 | 2047.00 | 0.9908 |
| Right Velocity | 7.38 | 264.67 | 0.0194 |
| Sonic Devc. Velocity | 0.33 | 1.00 | NA |
| Fifth-Wheel Velocity | -1.25 | 255.50 | 0.0195 |

CALIBRATION FILE: C1019D

| | <i>Zero Value</i> | <i>Shunt Value</i> | <i>Scale Value</i> |
|----------------------|-------------------|--------------------|--------------------|
| Left Vertical | -942.58 | 257.71 | 0.8723 |
| Left Longitudinal | -37.88 | 1165.42 | 0.8580 |
| Left Side | -399.04 | 1985.04 | 0.8959 |
| Left Velocity | 1.33 | 257.38 | 0.0195 |
| Right Vertical | -686.58 | 513.00 | 0.8853 |
| Right Longitudinal | 35.42 | 1237.75 | 0.8743 |
| Right Side | -371.75 | 2027.21 | 1.0000 |
| Right Velocity | 10.00 | 266.92 | 0.0195 |
| Sonic Devc. Velocity | 2.63 | 2.21 | NA |
| Fifth-Wheel Velocity | 1.13 | 257.67 | 0.0195 |

CALIBRATION FILE: C1019E

| | <i>Zero Value</i> | <i>Shunt Value</i> | <i>Scale Value</i> |
|----------------------|-------------------|--------------------|--------------------|
| Left Vertical | -943.83 | 255.63 | 0.8729 |
| Left Longitudinal | -43.54 | 1160.00 | 0.8580 |
| Left Side | -416.25 | 1969.88 | 0.8952 |
| Left Velocity | 3.00 | 259.08 | 0.0195 |
| Right Vertical | -688.04 | 511.42 | 0.8854 |
| Right Longitudinal | 28.67 | 1231.17 | 0.8740 |
| Right Side | -377.38 | 2014.92 | 1.0028 |
| Right Velocity | 10.96 | 268.71 | 0.0194 |
| Sonic Devc. Velocity | 4.17 | 3.88 | NA |
| Fifth-Wheel Velocity | 2.63 | 259.50 | 0.0195 |

CALIBRATION FILE: C1019F

| | <i>Zero Value</i> | <i>Shunt Value</i> | <i>Scale Value</i> |
|----------------------|-------------------|--------------------|--------------------|
| Left Vertical | -944.17 | 255.71 | 0.8726 |
| Left Longitudinal | -47.00 | 1157.08 | 0.8577 |
| Left Side | -383.96 | 2002.29 | 0.8951 |
| Left Velocity | 4.33 | 246.96 | 0.0207 |
| Right Vertical | -689.83 | 510.04 | 0.8851 |
| Right Longitudinal | 28.86 | 1231.92 | 0.8743 |
| Right Side | -353.38 | 2046.58 | 0.9997 |
| Right Velocity | 12.25 | 256.13 | 0.0205 |
| Sonic Devc. Velocity | 5.25 | 5.38 | NA |
| Fifth-Wheel Velocity | 3.46 | 247.54 | 0.0205 |

CALIBRATION FILE: C1019G

| | <i>Zero Value</i> | <i>Shunt Value</i> | <i>Scale Value</i> |
|----------------------|-------------------|--------------------|--------------------|
| Left Vertical | -942.88 | 257.25 | 0.8724 |
| Left Longitudinal | -57.17 | 1146.38 | 0.8578 |
| Left Side | -399.00 | 1988.67 | 0.8946 |
| Left Velocity | 57.67 | 254.00 | 0.0255 |
| Right Vertical | -689.38 | 510.42 | 0.8852 |
| Right Longitudinal | 18.17 | 1219.83 | 0.8737 |
| Right Side | -347.54 | 2047.00 | 1.0019 |
| Right Velocity | 66.04 | 262.92 | 0.0254 |
| Sonic Devc. Velocity | 5.71 | 6.17 | NA |
| Fifth-Wheel Velocity | 57.21 | 254.96 | 0.0253 |

CALIBRATION FILE: C1019H

| | <i>Zero Value</i> | <i>Shunt Value</i> | <i>Scale Value</i> |
|----------------------|-------------------|--------------------|--------------------|
| Left Vertical | -944.96 | 255.75 | 0.8720 |
| Left Longitudinal | -59.42 | 1148.33 | 0.8573 |
| Left Side | -403.71 | 1990.46 | 0.8922 |
| Left Velocity | 58.88 | 259.80 | 0.0249 |
| Right Vertical | -639.54 | 510.29 | 0.8851 |
| Right Longitudinal | 15.83 | 1219.00 | 0.8739 |
| Right Side | -340.67 | 2036.04 | 1.0094 |
| Right Velocity | 67.21 | 268.88 | 0.0248 |
| Sonic Devc. Velocity | 6.50 | 6.92 | NA |
| Fifth-Wheel Velocity | 57.67 | 260.17 | 0.0247 |

CALIBRATION FILE: C1019I

| | <i>Zero Value</i> | <i>Shunt Value</i> | <i>Scale Value</i> |
|----------------------|-------------------|--------------------|--------------------|
| Left Vertical | -945.00 | 255.08 | 0.8724 |
| Left Longitudinal | -54.96 | 1147.96 | 0.8578 |
| Left Side | -441.92 | 1948.08 | 0.8937 |
| Left Velocity | 6.63 | 262.54 | 0.0195 |
| Right Vertical | -691.63 | 508.00 | 0.8853 |
| Right Longitudinal | -30.67 | 1171.88 | 0.8737 |
| Right Side | -380.25 | 2037.83 | 0.9921 |
| Right Velocity | 14.50 | 272.21 | 0.0194 |
| Sonic Devc. Velocity | 6.92 | 7.38 | NA |
| Fifth-Wheel Velocity | 5.29 | 262.29 | 0.0195 |

CALIBRATION FILE: C1019J

| | <i>Zero Value</i> | <i>Shunt Value</i> | <i>Scale Value</i> |
|----------------------|-------------------|--------------------|--------------------|
| Left Vertical | -945.63 | 255.25 | 0.8719 |
| Left Longitudinal | -42.42 | 1160.83 | 0.8576 |
| Left Side | -474.79 | 1913.71 | 0.8943 |
| Left Velocity | 7.29 | 268.63 | 0.0191 |
| Right Vertical | -692.33 | 506.75 | 0.8857 |
| Right Longitudinal | 22.42 | 1224.96 | 0.8741 |
| Right Side | -420.75 | 1966.92 | 1.0047 |
| Right Velocity | 14.86 | 277.21 | 0.0191 |
| Sonic Devc. Velocity | 7.38 | 7.42 | NA |
| Fifth-Wheel Velocity | 6.00 | 269.54 | 0.0190 |

CALIBRATION FILE: C1019K

| | <i>Zero Value</i> | <i>Shunt Value</i> | <i>Scale Value</i> |
|----------------------|-------------------|--------------------|--------------------|
| Left Vertical | -944.13 | 256.08 | 0.8723 |
| Left Longitudinal | -59.46 | 1144.25 | 0.8579 |
| Left Side | -400.63 | 1992.46 | 0.8926 |
| Left Velocity | 62.30 | 264.54 | 0.0247 |
| Right Vertical | -691.33 | 507.92 | 0.8856 |
| Right Longitudinal | 19.63 | 1221.54 | 0.8738 |
| Right Side | -345.29 | 2028.46 | 1.0106 |
| Right Velocity | 68.54 | 272.79 | 0.0245 |
| Sonic Devc. Velocity | 7.75 | 7.79 | NA |
| Fifth-Wheel Velocity | 59.75 | 265.08 | 0.0244 |

CALIBRATION FILE: C1019L

| | <i>Zero Value</i> | <i>Shunt Value</i> | <i>Scale Value</i> |
|----------------------|-------------------|--------------------|--------------------|
| Left Vertical | -944.08 | 255.79 | 0.8726 |
| Left Longitudinal | -36.00 | 1167.29 | 0.8579 |
| Left Side | -450.75 | 1938.46 | 0.8940 |
| Left Velocity | 7.75 | 259.50 | 0.0199 |
| Right Vertical | -692.42 | 507.04 | 0.8854 |
| Right Longitudinal | 39.50 | 1242.21 | 0.8741 |
| Right Side | -401.88 | 1977.08 | 1.0084 |
| Right Velocity | 15.42 | 267.67 | 0.0198 |
| Sonic Devc. Velocity | 8.17 | 8.88 | NA |
| Fifth-Wheel Velocity | 6.79 | 260.38 | 0.0197 |

CALIBRATION FILE: C1019M

| | <i>Zero Value</i> | <i>Shunt Value</i> | <i>Scale Value</i> |
|----------------------|-------------------|--------------------|--------------------|
| Left Vertical | -946.71 | 253.5 | 0.8723 |
| Left Longitudinal | -53.96 | 1148.83 | 0.8578 |
| Left Side | -452.54 | 1940.13 | 0.8927 |
| Left Velocity | 8.04 | 268.25 | 0.0192 |
| Right Vertical | -695.79 | 503.54 | 0.8855 |
| Right Longitudinal | -30.79 | 1171.79 | 0.8741 |
| Right Side | -381.92 | 2005.79 | 1.0047 |
| Right Velocity | 15.79 | 276.54 | 0.0192 |
| Sonic Devc. Velocity | 8.54 | 8.58 | NA |
| Fifth-Wheel Velocity | 7.13 | 268.88 | 0.0191 |

CALIBRATION FILE: C10190

| | <i>Zero Value</i> | <i>Shunt Value</i> | <i>Scale Value</i> |
|----------------------|-------------------|--------------------|--------------------|
| Left Vertical | -945.42 | 254.92 | 0.8723 |
| Left Longitudinal | -53.50 | 1149.54 | 0.8577 |
| Left Side | -452.33 | 1941.00 | 0.8925 |
| Left Velocity | 7.83 | 261.13 | 0.0197 |
| Right Vertical | -696.08 | 503.54 | 0.8853 |
| Right Longitudinal | -30.63 | 1171.88 | 0.8738 |
| Right Side | -382.08 | 2003.38 | 1.0057 |
| Right Velocity | 15.79 | 269.92 | 0.0197 |
| Sonic Devc. Velocity | 8.25 | 8.42 | NA |
| Fifth-Wheel Velocity | 7.21 | 262.21 | 0.0196 |

CALIBRATION FILE: C1019P

| | <i>Zero Value</i> | <i>Shunt Value</i> | <i>Scale Value</i> |
|----------------------|-------------------|--------------------|--------------------|
| Left Vertical | -944.04 | 255.88 | 0.8726 |
| Left Longitudinal | -53.54 | 1147.63 | 0.8576 |
| Left Side | -412.50 | 1983.33 | 0.8915 |
| Left Velocity | 59.13 | 264.83 | 0.0243 |
| Right Vertical | -695.04 | 504.00 | 0.8857 |
| Right Longitudinal | 13.96 | 1217.33 | 0.8741 |
| Right Side | -338.83 | 2033.92 | 1.0111 |
| Right Velocity | 67.00 | 273.71 | 0.0242 |
| Sonic Devc. Velocity | 8.79 | 8.71 | NA |
| Fifth-Wheel Velocity | 58.13 | 265.75 | 0.0241 |

CALIBRATION FILE: C1019Q

| | <i>Zero Value</i> | <i>Shunt Value</i> | <i>Scale Value</i> |
|----------------------|-------------------|--------------------|--------------------|
| Left Vertical | -943.86 | 256.46 | 0.8723 |
| Left Longitudinal | -58.63 | 1145.54 | 0.8577 |
| Left Side | -399.33 | 1993.88 | 0.8925 |
| Left Velocity | 67.71 | 258.75 | 0.0262 |
| Right Vertical | -695.96 | 502.88 | 0.8859 |
| Right Longitudinal | 18.50 | 1222.75 | 0.8741 |
| Right Side | -348.67 | 2019.38 | 1.0131 |
| Right Velocity | 75.54 | 267.38 | 0.0261 |
| Sonic Devc. Velocity | 8.67 | 8.67 | NA |
| Fifth-Wheel Velocity | 67.63 | 258.00 | 0.0263 |

CALIBRATION FILE: C1019R

| | <i>Zero Value</i> | <i>Shunt Value</i> | <i>Scale Value</i> |
|----------------------|-------------------|--------------------|--------------------|
| Left Vertical | -944.58 | 255.92 | 0.8721 |
| Left Longitudinal | -62.08 | 1143.42 | 0.8578 |
| Left Side | -411.67 | 1988.0 | 0.8901 |
| Left Velocity | 62.42 | 264.38 | 0.0248 |
| Right Vertical | -695.79 | 503.67 | 0.8854 |
| Right Longitudinal | 21.25 | 1224.63 | 0.8740 |
| Right Side | -351.83 | 2029.79 | 1.0073 |
| Right Velocity | 70.46 | 272.17 | 0.0248 |
| Sonic Devc. Velocity | 9.0 | 9.08 | NA |
| Fifth-Wheel Velocity | 61.58 | 265.92 | 0.0245 |

CALIBRATION FILE: C1019S

| | <i>Zero Value</i> | <i>Shunt Value</i> | <i>Scale Value</i> |
|----------------------|-------------------|--------------------|--------------------|
| Left Vertical | -944.67 | 255.54 | 0.8723 |
| Left Longitudinal | -55.58 | 1147.54 | 0.8579 |
| Left Side | -455.67 | 1937.71 | 0.8925 |
| Left Velocity | 8.04 | 263.96 | 0.0195 |
| Right Vertical | -695.08 | 504.00 | 0.8857 |
| Right Longitudinal | -28.67 | 1174.13 | 0.8743 |
| Right Side | -380.67 | 2004.38 | 1.0059 |
| Right Velocity | 16.04 | 270.29 | 0.0197 |
| Sonic Devc. Velocity | 9.04 | 9.17 | NA |
| Fifth-Wheel Velocity | 7.17 | 265.71 | 0.0193 |

CALIBRATION FILE: C1019T

| | <i>Zero Value</i> | <i>Shunt Value</i> | <i>Scale Value</i> |
|----------------------|-------------------|--------------------|--------------------|
| Left Vertical | -944.83 | 255.29 | 0.8724 |
| Left Longitudinal | -60.08 | 1143.00 | 0.8582 |
| Left Side | -404.13 | 1984.04 | 0.8944 |
| Left Velocity | 57.58 | 258.96 | 0.0248 |
| Right Vertical | -696.63 | 502.63 | 0.8856 |
| Right Longitudinal | 21.96 | 1219.25 | 0.8739 |
| Right Side | -353.50 | 2022.38 | 1.0097 |
| Right Velocity | 66.21 | 269.00 | 0.0247 |
| Sonic Devc. Velocity | 9.08 | 8.50 | NA |
| Fifth-Wheel Velocity | 58.21 | 260.17 | 0.0248 |

CALIBRATION FILE: C1019U

| | <i>Zero Value</i> | <i>Shunt Value</i> | <i>Scale Value</i> |
|----------------------|-------------------|--------------------|--------------------|
| Left Vertical | -943.63 | 256.25 | 0.8726 |
| Left Longitudinal | -42.79 | 1160.46 | 0.8577 |
| Left Side | -420.88 | 1969.63 | 0.8935 |
| Left Velocity | 7.25 | 261.46 | 0.0197 |
| Right Vertical | -695.38 | 502.83 | 0.8863 |
| Right Longitudinal | 25.17 | 1227.96 | 0.8738 |
| Right Side | -370.17 | 2009.38 | 1.0082 |
| Right Velocity | 14.79 | 270.88 | 0.0195 |
| Sonic Devc. Velocity | 8.17 | 8.33 | NA |
| Fifth-Wheel Velocity | 6.67 | 261.08 | 0.0197 |

CALIBRATION FILE: C1019V

| | <i>Zero Value</i> | <i>Shunt Value</i> | <i>Scale Value</i> |
|----------------------|-------------------|--------------------|--------------------|
| Left Vertical | -944.50 | 255.79 | 0.8723 |
| Left Longitudinal | -54.79 | 1148.13 | 0.8574 |
| Left Side | -454.13 | 1938.46 | 0.8928 |
| Left Velocity | 7.00 | 251.08 | 0.0205 |
| Right Vertical | -696.38 | 502.58 | 0.8858 |
| Right Longitudinal | -28.96 | 1173.42 | 0.8739 |
| Right Side | -381.96 | 2000.67 | 1.0069 |
| Right Velocity | 15.21 | 260.17 | 0.0204 |
| Sonic Devc. Velocity | 7.83 | 7.50 | NA |
| Fifth-Wheel Velocity | 6.67 | 251.58 | 0.0204 |

REPORT DOCUMENTATION PAGE

Form Approved
OMB No. 0704-0188

Public reporting burden for this collection of information is estimated to average 1 hour per response, including the time for reviewing instructions, searching existing data sources, gathering and maintaining the data needed, and completing and reviewing the collection of information. Send comments regarding this burden estimate or any other aspect of this collection of information, including suggestion for reducing this burden, to Washington Headquarters Services, Directorate for Information Operations and Reports, 1215 Jefferson Davis Highway, Suite 1204, Arlington, VA 22202-4302, and to the Office of Management and Budget, Paperwork Reduction Project (0704-0188), Washington, DC 20503.

| | | | | | |
|--|--|--|--|---|--|
| 1. AGENCY USE ONLY (Leave blank) | | 2. REPORT DATE <p style="text-align: center;">April 1992</p> | | 3. REPORT TYPE AND DATES COVERED | |
| 4. TITLE AND SUBTITLE <p style="text-align: center;">Precision Analysis and Recommended Test Procedures for Mobility Measurements Made with an Instrumented Vehicle</p> | | | | 5. FUNDING NUMBERS <p>PE: 6.27.84A PR: 4A762784AT42 TA: CS WU: 007</p> | |
| 6. AUTHORS <p style="text-align: center;">Sally A. Shoop</p> | | | | | |
| 7. PERFORMING ORGANIZATION NAME(S) AND ADDRESS(ES) <p>U.S. Army Cold Regions Research and Engineering Laboratory 72 Lyme Road Hanover, N.H. 03755-1290</p> | | | | 8. PERFORMING ORGANIZATION REPORT NUMBER <p style="text-align: center;">Special Report 92-7</p> | |
| 9. SPONSORING/MONITORING AGENCY NAME(S) AND ADDRESS(ES) <p>Office of the Chief of Engineers Washington, D.C. 20314-1000</p> | | | | 10. SPONSORING/MONITORING AGENCY REPORT NUMBER | |
| 11. SUPPLEMENTARY NOTES | | | | | |
| 12a. DISTRIBUTION/AVAILABILITY STATEMENT <p>Approved for public release; distribution is unlimited.</p> <p>Available from NTIS, Springfield, Virginia 22161.</p> | | | | 12b. DISTRIBUTION CODE | |
| 13. ABSTRACT (<i>Maximum 200 words</i>) <p>This report addresses the precision of mobility measurements made using an instrumented vehicle. Systematic errors were documented and new techniques established to eliminate or minimize these errors. An increase in the precision and accuracy of mobility measurements will allow the successful pursuit of new research efforts of concern to cold regions mobility, such as the resistance measurements of trailing tires and terrain resistance on shallow snow or winter soils. Systematic errors due to calibration methods, temperature, vehicle speed and weight distribution were observed and quantified. Based on these results, suggested techniques to eliminate or minimize these errors and improve precision are as follows. 1) The method of calibration (air, static or rolling) should be chosen based on the objective of the experiment. Calibrating the vehicle while it is rolling yields the most consistent results from test to test; however, a static calibration is needed to measure the total resistance of the vehicle running gear. 2) Because of the wide range of temperatures considered in cold regions testing and the temperature sensitivity of the equipment, the vehicle and all equipment should be operating and temperatures stabilized before vehicle calibration and testing begins. If the weather changes significantly during the course of the tests, it should be noted and the vehicle should be recalibrated. 3) The vehicle must be on as level and smooth a surface as possible because the load on the wheels is extremely sensitive to weight distribution (and tilt) of the vehicle. Small variations in the weight distribution are also reflected in the contact area of the tires. 4) Mobility testing procedures should routinely include a hard surface motion resistance measurement for each set of test conditions to serve as a reference for the terrain mobility measurements and as a comparison between data sets.</p> | | | | | |
| 14. SUBJECT TERMS <p style="text-align: center;">Experimental error Vehicle mobility Statistical analysis</p> | | | | 15. NUMBER OF PAGES <p style="text-align: center;">54</p> | |
| | | | | 16. PRICE CODE | |
| 17. SECURITY CLASSIFICATION OF REPORT <p style="text-align: center;">UNCLASSIFIED</p> | | 18. SECURITY CLASSIFICATION OF THIS PAGE <p style="text-align: center;">UNCLASSIFIED</p> | | 19. SECURITY CLASSIFICATION OF ABSTRACT <p style="text-align: center;">UNCLASSIFIED</p> | |
| | | | | 20. LIMITATION OF ABSTRACT <p style="text-align: center;">UL</p> | |